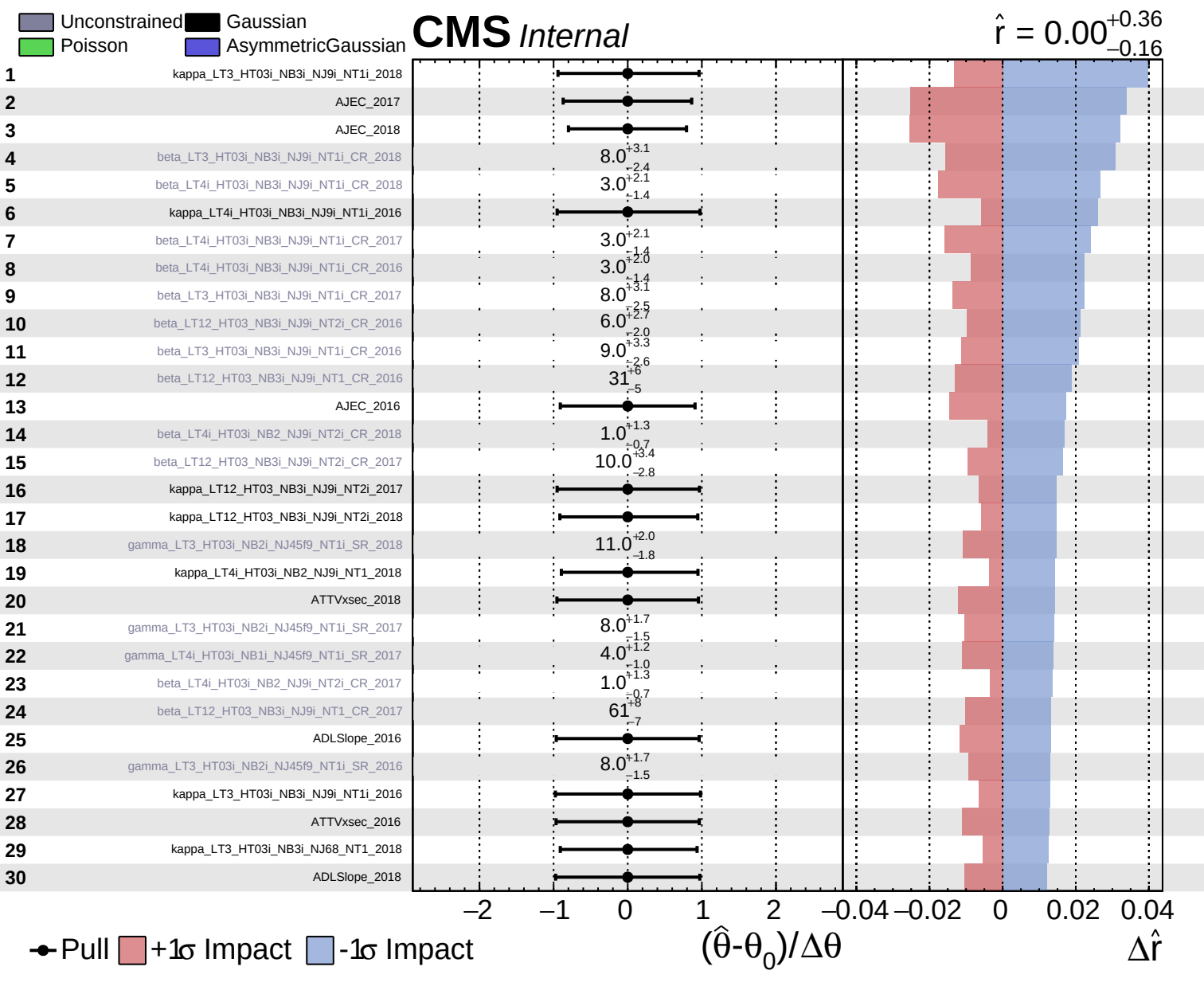
Unconstrained
Gaussian
Poisson
AsymmetricGaussian
CMS Internal
r̂ = 0.00 +0.36 −0.16
1 kappa_LT3_HT03i_NB3i_NJ9i_NT1i_2018
2 AJEC_2017
3 AJEC_2018
4 beta_LT3_HT03i_NB3i_NJ9i_NT1i_CR_2018 8.0 +3.1 −2.4
5 beta_LT4i_HT03i_NB3i_NJ9i_NT1i_CR_2018 3.0 +2.1 −1.4
6 kappa_LT4i_HT03i_NB3i_NJ9i_NT1i_2016
7 beta_LT4i_HT03i_NB3i_NJ9i_NT1i_CR_2017 3.0 +2.1 −1.4
8 beta_LT4i_HT03i_NB3i_NJ9i_NT1i_CR_2016 3.0 +2.0 −1.4
9 beta_LT3_HT03i_NB3i_NJ9i_NT1i_CR_2017 8.0 +3.1 −2.5
10 beta_LT12_HT03_NB3i_NJ9i_NT2i_CR_2016 6.0 +2.7 −2.0
11 beta_LT3_HT03i_NB3i_NJ9i_NT1i_CR_2016 9.0 +3.3 −2.6
12 beta_LT12_HT03_NB3i_NJ9i_NT1_CR_2016 31 +6 −5
13 AJEC_2016
14 beta_LT4i_HT03i_NB2_NJ9i_NT2i_CR_2018 1.0 +1.3 −0.7
15 beta_LT12_HT03_NB3i_NJ9i_NT2i_CR_2017 10.0 +3.4 −2.8
16 kappa_LT12_HT03_NB3i_NJ9i_NT2i_2017
17 kappa_LT12_HT03_NB3i_NJ9i_NT2i_2018
18 gamma_LT3_HT03i_NB2i_NJ45f9_NT1i_SR_2018 11.0 +2.0 −1.8
19 kappa_LT4i_HT03i_NB2_NJ9i_NT1_2018
20 ATTVxsec_2018
21 gamma_LT3_HT03i_NB2i_NJ45f9_NT1i_SR_2017 8.0 +1.7 −1.5
22 gamma_LT4i_HT03i_NB1i_NJ45f9_NT1i_SR_2017 4.0 +1.2 −1.0
23 beta_LT4i_HT03i_NB2_NJ9i_NT2i_CR_2017 1.0 +1.3 −0.7
24 beta_LT12_HT03_NB3i_NJ9i_NT1_CR_2017 61 +8 −7
25 ADLSlope_2016
26 gamma_LT3_HT03i_NB2i_NJ45f9_NT1i_SR_2016 8.0 +1.7 −1.5
27 kappa_LT3_HT03i_NB3i_NJ9i_NT1i_2016
28 ATTVxsec_2016
29 kappa_LT3_HT03i_NB3i_NJ68_NT1_2018
30 ADLSlope_2018
−2 −1 0 1 2
−0.04 −0.02 0 0.02 0.04
Pull
+1σ Impact
-1σ Impact
(θ̂-θ0)/Δθ
Δr̂

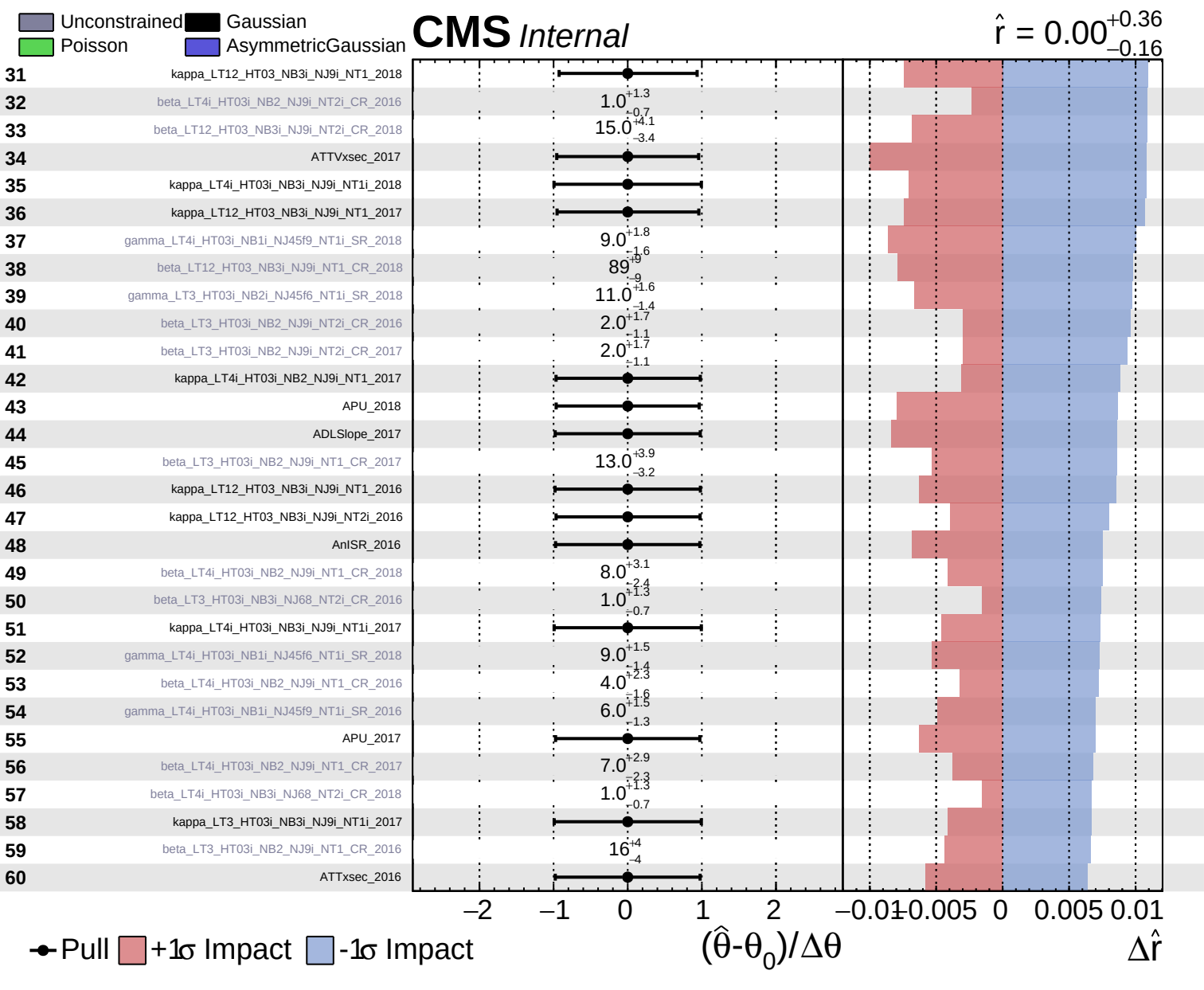
Unconstrained
Gaussian
Poisson
AsymmetricGaussian
CMS Internal
r̂ = 0.00 +0.36 −0.16
31 kappa_LT12_HT03_NB3i_NJ9i_NT1_2018
32 beta_LT4i_HT03i_NB2_NJ9i_NT2i_CR_2016
33 beta_LT12_HT03_NB3i_NJ9i_NT2i_CR_2018
34 ATTVxsec_2017
35 kappa_LT4i_HT03i_NB3i_NJ9i_NT1i_2018
36 kappa_LT12_HT03_NB3i_NJ9i_NT1_2017
37 gamma_LT4i_HT03i_NB1i_NJ45f9_NT1i_SR_2018
38 beta_LT12_HT03_NB3i_NJ9i_NT1_CR_2018
39 gamma_LT3_HT03i_NB2i_NJ45f6_NT1i_SR_2018
40 beta_LT3_HT03i_NB2_NJ9i_NT2i_CR_2016
41 beta_LT3_HT03i_NB2_NJ9i_NT2i_CR_2017
42 kappa_LT4i_HT03i_NB2_NJ9i_NT1_2017
43 APU_2018
44 ADLSlope_2017
45 beta_LT3_HT03i_NB2_NJ9i_NT1_CR_2017
46 kappa_LT12_HT03_NB3i_NJ9i_NT1_2016
47 kappa_LT12_HT03_NB3i_NJ9i_NT2i_2016
48 AnISR_2016
49 beta_LT4i_HT03i_NB2_NJ9i_NT1_CR_2018
50 beta_LT3_HT03i_NB3i_NJ68_NT2i_CR_2016
51 kappa_LT4i_HT03i_NB3i_NJ9i_NT1i_2017
52 gamma_LT4i_HT03i_NB1i_NJ45f6_NT1i_SR_2018
53 beta_LT4i_HT03i_NB2_NJ9i_NT1_CR_2016
54 gamma_LT4i_HT03i_NB1i_NJ45f9_NT1i_SR_2016
55 APU_2017
56 beta_LT4i_HT03i_NB2_NJ9i_NT1_CR_2017
57 beta_LT4i_HT03i_NB3i_NJ68_NT2i_CR_2018
58 kappa_LT3_HT03i_NB3i_NJ9i_NT1i_2017
59 beta_LT3_HT03i_NB2_NJ9i_NT1_CR_2016
60 ATTxsec_2016
1.0 +1.3 −0.7
15.0 +4.1 −3.4
9.0 +1.8 −1.6
89 +9 −9
11.0 +1.6 −1.4
2.0 +1.7 −1.1
2.0 +1.7 −1.1
13.0 +3.9 −3.2
8.0 +3.1 −2.4
1.0 +1.3 −0.7
9.0 +1.5 −1.4
4.0 +2.3 −1.6
6.0 +1.5 −1.3
7.0 +2.9 −2.3
1.0 +1.3 −0.7
16 +4 −4
−2 −1 0 1 2
−0.01 −0.005 0 0.005 0.01
Pull
+1σ Impact
-1σ Impact
(θ̂-θ0)/Δθ
Δr̂

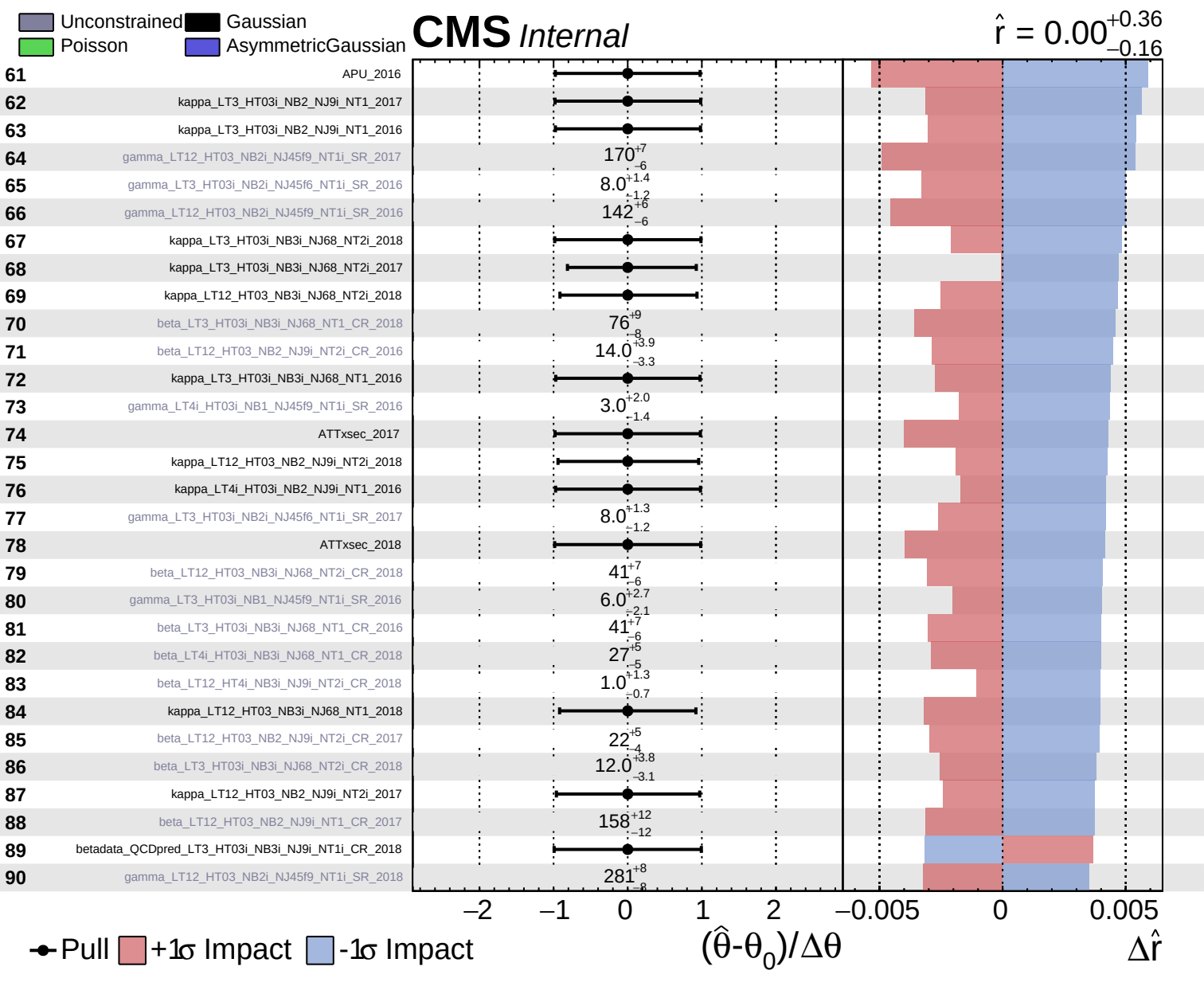
Unconstrained
Gaussian
Poisson
AsymmetricGaussian
CMS Internal
r̂ = 0.00 +0.36 −0.16
61 APU_2016
62 kappa_LT3_HT03i_NB2_NJ9i_NT1_2017
63 kappa_LT3_HT03i_NB2_NJ9i_NT1_2016
64 gamma_LT12_HT03_NB2i_NJ45f9_NT1i_SR_2017
65 gamma_LT3_HT03i_NB2i_NJ45f6_NT1i_SR_2016
66 gamma_LT12_HT03_NB2i_NJ45f9_NT1i_SR_2016
67 kappa_LT3_HT03i_NB3i_NJ68_NT2i_2018
68 kappa_LT3_HT03i_NB3i_NJ68_NT2i_2017
69 kappa_LT12_HT03_NB3i_NJ68_NT2i_2018
70 beta_LT3_HT03i_NB3i_NJ68_NT1_CR_2018
71 beta_LT12_HT03_NB2_NJ9i_NT2i_CR_2016
72 kappa_LT3_HT03i_NB3i_NJ68_NT1_2016
73 gamma_LT4i_HT03i_NB1_NJ45f9_NT1i_SR_2016
74 ATTxsec_2017
75 kappa_LT12_HT03_NB2_NJ9i_NT2i_2018
76 kappa_LT4i_HT03i_NB2_NJ9i_NT1_2016
77 gamma_LT3_HT03i_NB2i_NJ45f6_NT1i_SR_2017
78 ATTxsec_2018
79 beta_LT12_HT03_NB3i_NJ68_NT2i_CR_2018
80 gamma_LT3_HT03i_NB1_NJ45f9_NT1i_SR_2016
81 beta_LT3_HT03i_NB3i_NJ68_NT1_CR_2016
82 beta_LT4i_HT03i_NB3i_NJ68_NT1_CR_2018
83 beta_LT12_HT4i_NB3i_NJ9i_NT2i_CR_2018
84 kappa_LT12_HT03_NB3i_NJ68_NT1_2018
85 beta_LT12_HT03_NB2_NJ9i_NT2i_CR_2017
86 beta_LT3_HT03i_NB3i_NJ68_NT2i_CR_2018
87 kappa_LT12_HT03_NB2_NJ9i_NT2i_2017
88 beta_LT12_HT03_NB2_NJ9i_NT1_CR_2017
89 betadata_QCDpred_LT3_HT03i_NB3i_NJ9i_NT1i_CR_2018
90 gamma_LT12_HT03_NB2i_NJ45f9_NT1i_SR_2018
170 +7 −6
8.0 +1.4 −1.2
142 +6 −6
76 +9 −8
14.0 +3.9 −3.3
3.0 +2.0 −1.4
8.0 +1.3 −1.2
41 +7 −6
6.0 +2.7 −2.1
41 +7 −6
27 +5 −5
1.0 +1.3 −0.7
22 +5 −4
12.0 +3.8 −3.1
158 +12 −12
281 +8 −8
−2
−1
0
1
2
−0.005
0
0.005
Pull
+1σ Impact
-1σ Impact
(θ̂-θ0)/Δθ
Δr̂

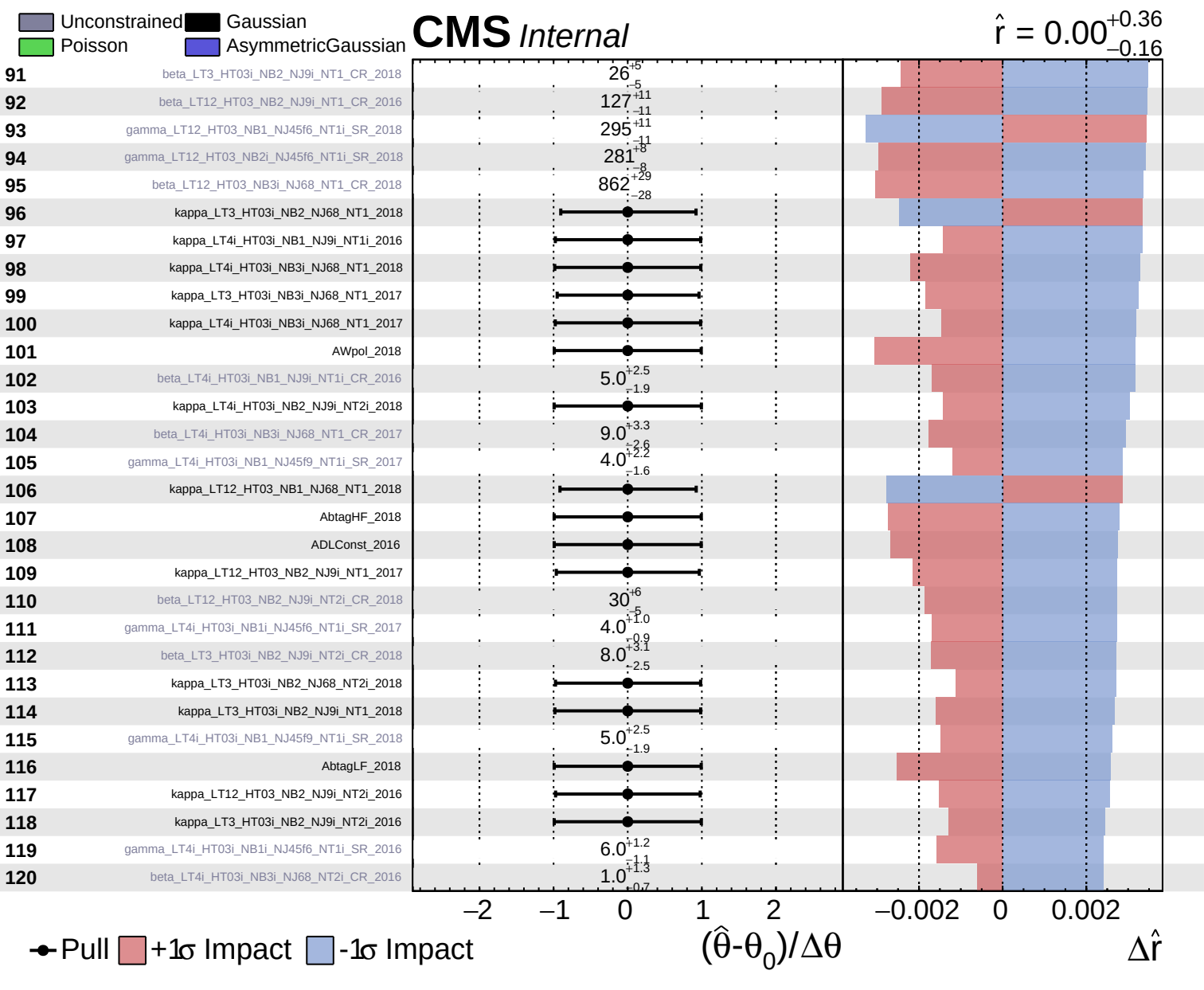
Unconstrained
Gaussian
Poisson
AsymmetricGaussian
CMS Internal
r̂ = 0.00 +0.36 −0.16
91 beta_LT3_HT03i_NB2_NJ9i_NT1_CR_2018
92 beta_LT12_HT03_NB2_NJ9i_NT1_CR_2016
93 gamma_LT12_HT03_NB1_NJ45f6_NT1i_SR_2018
94 gamma_LT12_HT03_NB2i_NJ45f6_NT1i_SR_2018
95 beta_LT12_HT03_NB3i_NJ68_NT1_CR_2018
96 kappa_LT3_HT03i_NB2_NJ68_NT1_2018
97 kappa_LT4i_HT03i_NB1_NJ9i_NT1i_2016
98 kappa_LT4i_HT03i_NB3i_NJ68_NT1_2018
99 kappa_LT3_HT03i_NB3i_NJ68_NT1_2017
100 kappa_LT4i_HT03i_NB3i_NJ68_NT1_2017
101 AWpol_2018
102 beta_LT4i_HT03i_NB1_NJ9i_NT1i_CR_2016
103 kappa_LT4i_HT03i_NB2_NJ9i_NT2i_2018
104 beta_LT4i_HT03i_NB3i_NJ68_NT1_CR_2017
105 gamma_LT4i_HT03i_NB1_NJ45f9_NT1i_SR_2017
106 kappa_LT12_HT03_NB1_NJ68_NT1_2018
107 AbtagHF_2018
108 ADLConst_2016
109 kappa_LT12_HT03_NB2_NJ9i_NT1_2017
110 beta_LT12_HT03_NB2_NJ9i_NT2i_CR_2018
111 gamma_LT4i_HT03i_NB1i_NJ45f6_NT1i_SR_2017
112 beta_LT3_HT03i_NB2_NJ9i_NT2i_CR_2018
113 kappa_LT3_HT03i_NB2_NJ68_NT2i_2018
114 kappa_LT3_HT03i_NB2_NJ9i_NT1_2018
115 gamma_LT4i_HT03i_NB1_NJ45f9_NT1i_SR_2018
116 AbtagLF_2018
117 kappa_LT12_HT03_NB2_NJ9i_NT2i_2016
118 kappa_LT3_HT03i_NB2_NJ9i_NT2i_2016
119 gamma_LT4i_HT03i_NB1i_NJ45f6_NT1i_SR_2016
120 beta_LT4i_HT03i_NB3i_NJ68_NT2i_CR_2016
26 +5 −5
127 +11 −11
295 +11 −11
281 +8 −8
862 +29 −28
5.0 +2.5 −1.9
9.0 +3.3 −2.6
4.0 +2.2 −1.6
30 +6 −5
4.0 +1.0 −0.9
8.0 +3.1 −2.5
5.0 +2.5 −1.9
6.0 +1.2 −1.1
1.0 +1.3 −0.7
−2
−1
0
1
2
−0.002
0
0.002
Pull
+1σ Impact
-1σ Impact
(θ̂-θ0)/Δθ
Δr̂

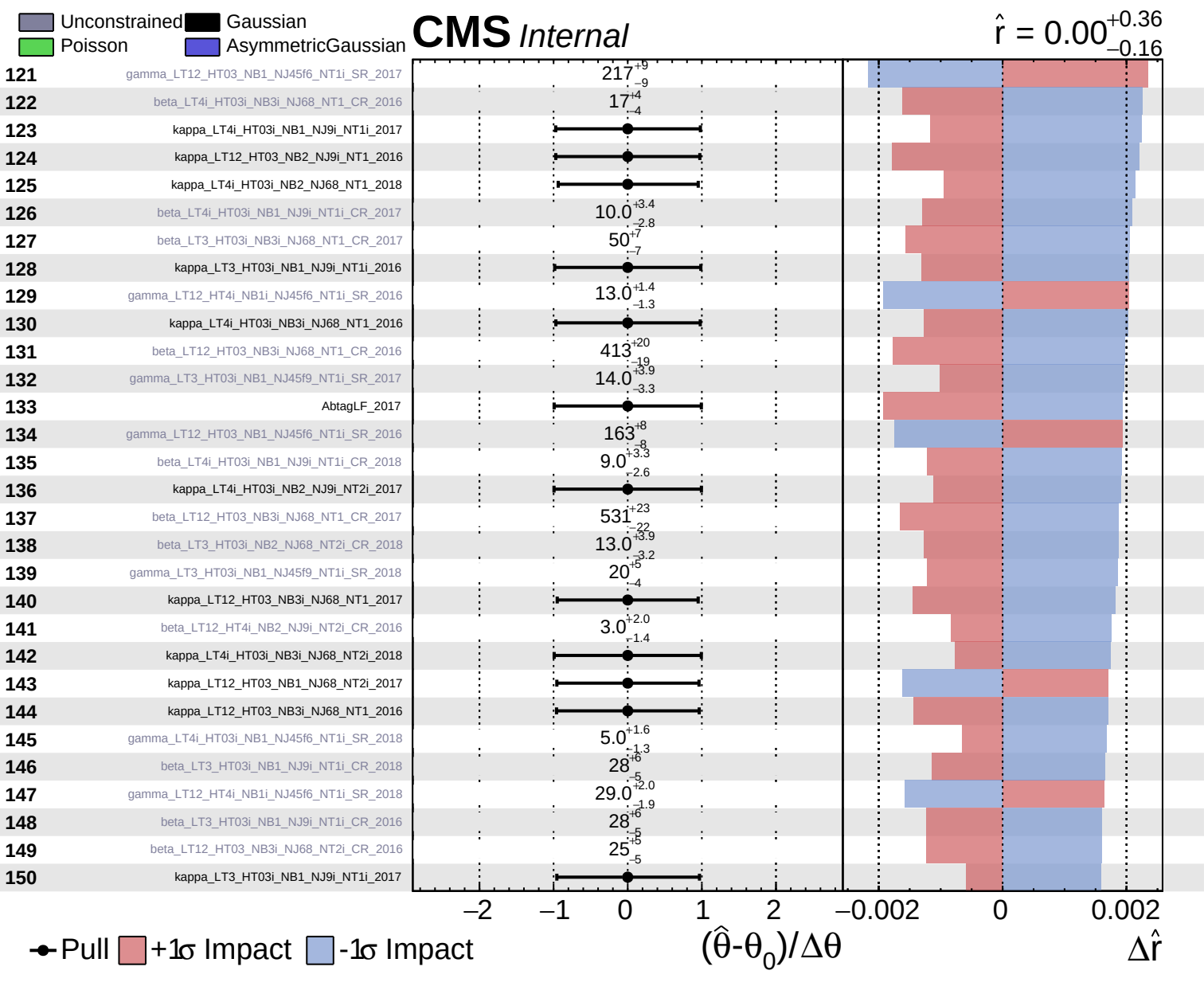
Unconstrained
Gaussian
Poisson
AsymmetricGaussian
CMS Internal
r̂ = 0.00 +0.36 −0.16
121 gamma_LT12_HT03_NB1_NJ45f6_NT1i_SR_2017
122 beta_LT4i_HT03i_NB3i_NJ68_NT1_CR_2016
123 kappa_LT4i_HT03i_NB1_NJ9i_NT1i_2017
124 kappa_LT12_HT03_NB2_NJ9i_NT1_2016
125 kappa_LT4i_HT03i_NB2_NJ68_NT1_2018
126 beta_LT4i_HT03i_NB1_NJ9i_NT1i_CR_2017
127 beta_LT3_HT03i_NB3i_NJ68_NT1_CR_2017
128 kappa_LT3_HT03i_NB1_NJ9i_NT1i_2016
129 gamma_LT12_HT4i_NB1i_NJ45f6_NT1i_SR_2016
130 kappa_LT4i_HT03i_NB3i_NJ68_NT1_2016
131 beta_LT12_HT03_NB3i_NJ68_NT1_CR_2016
132 gamma_LT3_HT03i_NB1_NJ45f9_NT1i_SR_2017
133 AbtagLF_2017
134 gamma_LT12_HT03_NB1_NJ45f6_NT1i_SR_2016
135 beta_LT4i_HT03i_NB1_NJ9i_NT1i_CR_2018
136 kappa_LT4i_HT03i_NB2_NJ9i_NT2i_2017
137 beta_LT12_HT03_NB3i_NJ68_NT1_CR_2017
138 beta_LT3_HT03i_NB2_NJ68_NT2i_CR_2018
139 gamma_LT3_HT03i_NB1_NJ45f9_NT1i_SR_2018
140 kappa_LT12_HT03_NB3i_NJ68_NT1_2017
141 beta_LT12_HT4i_NB2_NJ9i_NT2i_CR_2016
142 kappa_LT4i_HT03i_NB3i_NJ68_NT2i_2018
143 kappa_LT12_HT03_NB1_NJ68_NT2i_2017
144 kappa_LT12_HT03_NB3i_NJ68_NT1_2016
145 gamma_LT4i_HT03i_NB1_NJ45f6_NT1i_SR_2018
146 beta_LT3_HT03i_NB1_NJ9i_NT1i_CR_2018
147 gamma_LT12_HT4i_NB1i_NJ45f6_NT1i_SR_2018
148 beta_LT3_HT03i_NB1_NJ9i_NT1i_CR_2016
149 beta_LT12_HT03_NB3i_NJ68_NT2i_CR_2016
150 kappa_LT3_HT03i_NB1_NJ9i_NT1i_2017
217 +9 −9
17 +4 −4
10.0 +3.4 −2.8
50 +7 −7
13.0 +1.4 −1.3
413 +20 −19
14.0 +3.9 −3.3
163 +8 −8
9.0 +3.3 −2.6
531 +23 −22
13.0 +3.9 −3.2
20 +5 −4
3.0 +2.0 −1.4
5.0 +1.6 −1.3
28 +6 −5
29.0 +2.0 −1.9
28 +6 −5
25 +5 −5
−2
−1
0
1
2
(θ̂-θ0)/Δθ
−0.002
0
0.002
Δr̂
Pull
+1σ Impact
-1σ Impact

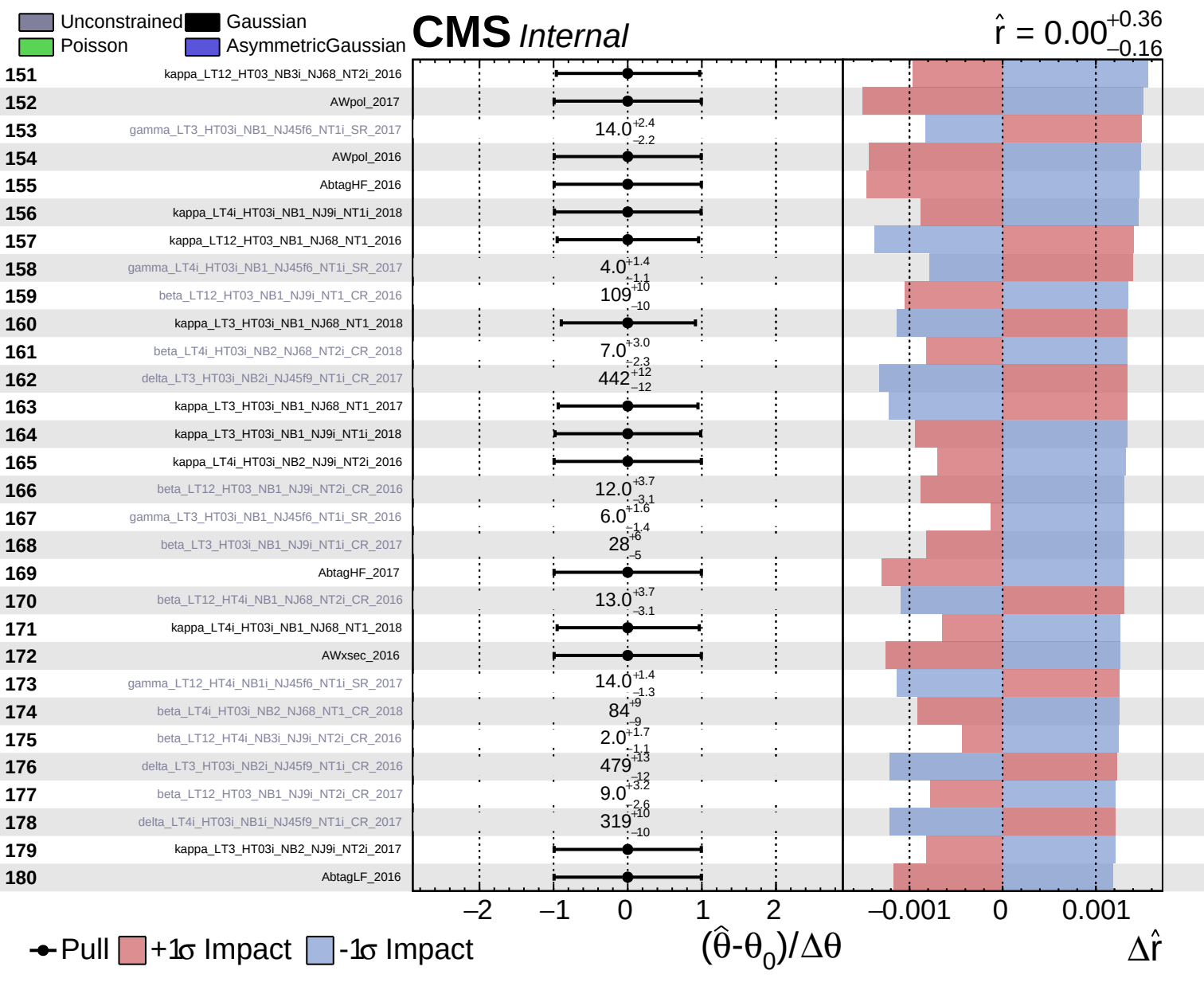
Unconstrained
Gaussian
Poisson
AsymmetricGaussian
CMS Internal
r̂ = 0.00 +0.36 −0.16
151 kappa_LT12_HT03_NB3i_NJ68_NT2i_2016
152 AWpol_2017
153 gamma_LT3_HT03i_NB1_NJ45f6_NT1i_SR_2017
154 AWpol_2016
155 AbtagHF_2016
156 kappa_LT4i_HT03i_NB1_NJ9i_NT1i_2018
157 kappa_LT12_HT03_NB1_NJ68_NT1_2016
158 gamma_LT4i_HT03i_NB1_NJ45f6_NT1i_SR_2017
159 beta_LT12_HT03_NB1_NJ9i_NT1_CR_2016
160 kappa_LT3_HT03i_NB1_NJ68_NT1_2018
161 beta_LT4i_HT03i_NB2_NJ68_NT2i_CR_2018
162 delta_LT3_HT03i_NB2i_NJ45f9_NT1i_CR_2017
163 kappa_LT3_HT03i_NB1_NJ68_NT1_2017
164 kappa_LT3_HT03i_NB1_NJ9i_NT1i_2018
165 kappa_LT4i_HT03i_NB2_NJ9i_NT2i_2016
166 beta_LT12_HT03_NB1_NJ9i_NT2i_CR_2016
167 gamma_LT3_HT03i_NB1_NJ45f6_NT1i_SR_2016
168 beta_LT3_HT03i_NB1_NJ9i_NT1i_CR_2017
169 AbtagHF_2017
170 beta_LT12_HT4i_NB1_NJ68_NT2i_CR_2016
171 kappa_LT4i_HT03i_NB1_NJ68_NT1_2018
172 AWxsec_2016
173 gamma_LT12_HT4i_NB1i_NJ45f6_NT1i_SR_2017
174 beta_LT4i_HT03i_NB2_NJ68_NT1_CR_2018
175 beta_LT12_HT4i_NB3i_NJ9i_NT2i_CR_2016
176 delta_LT3_HT03i_NB2i_NJ45f9_NT1i_CR_2016
177 beta_LT12_HT03_NB1_NJ9i_NT2i_CR_2017
178 delta_LT4i_HT03i_NB1i_NJ45f9_NT1i_CR_2017
179 kappa_LT3_HT03i_NB2_NJ9i_NT2i_2017
180 AbtagLF_2016
14.0 +2.4 −2.2
4.0 +1.4 −1.1
109 +10 −10
7.0 +3.0 −2.3
442 +12 −12
12.0 +3.7 −3.1
6.0 +1.6 −1.4
28 +6 −5
13.0 +3.7 −3.1
14.0 +1.4 −1.3
84 +9 −9
2.0 +1.7 −1.1
479 +13 −12
9.0 +3.2 −2.6
319 +10 −10
−2
−1
0
1
2
−0.001
0
0.001
Pull
+1σ Impact
-1σ Impact
(θ̂-θ0)/Δθ
Δr̂

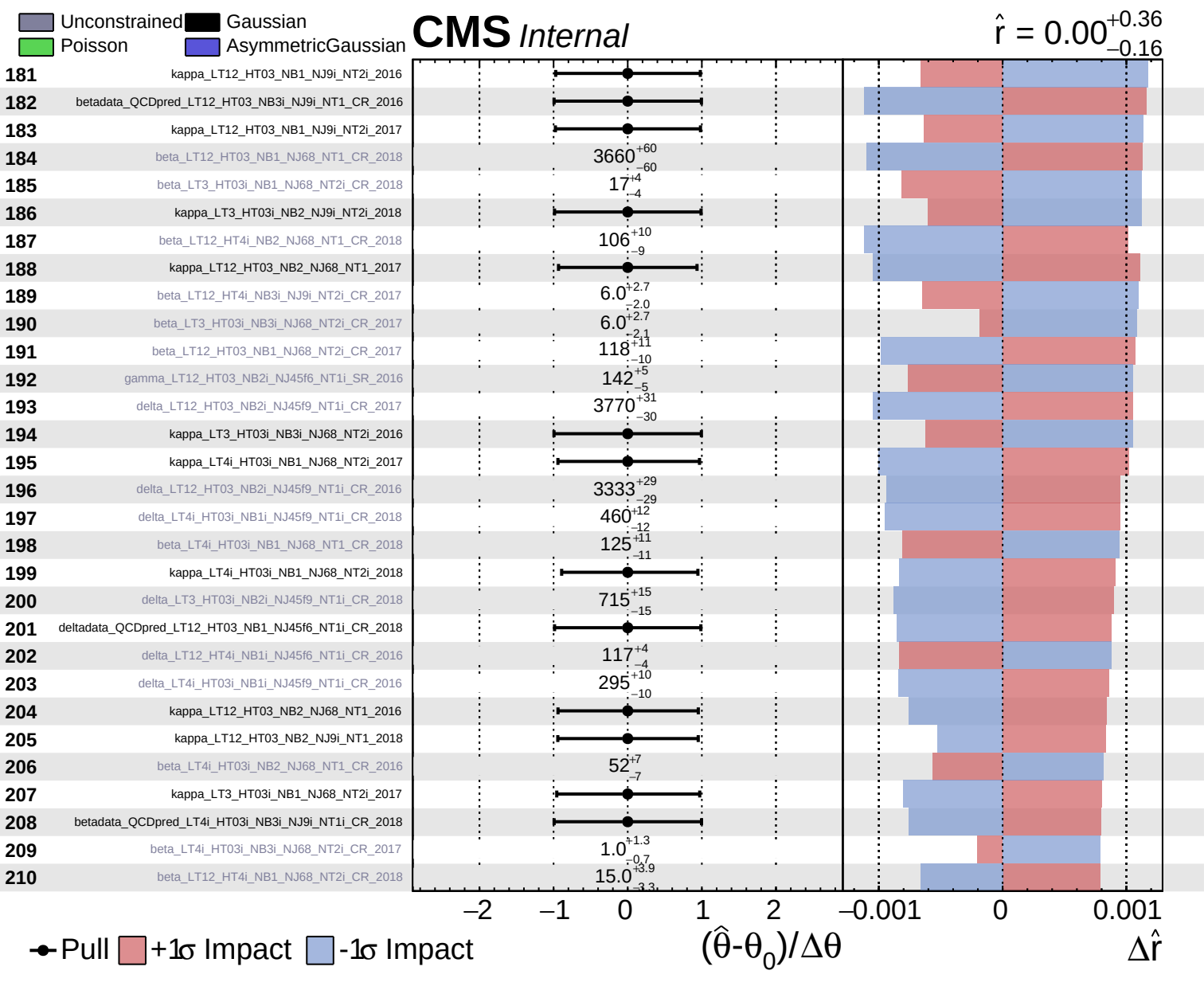
Unconstrained
Gaussian
Poisson
AsymmetricGaussian
CMS Internal
r̂ = 0.00 +0.36 −0.16
181 kappa_LT12_HT03_NB1_NJ9i_NT2i_2016
182 betadata_QCDpred_LT12_HT03_NB3i_NJ9i_NT1_CR_2016
183 kappa_LT12_HT03_NB1_NJ9i_NT2i_2017
184 beta_LT12_HT03_NB1_NJ68_NT1_CR_2018
3660 +60 −60
185 beta_LT3_HT03i_NB1_NJ68_NT2i_CR_2018
17 +4 −4
186 kappa_LT3_HT03i_NB2_NJ9i_NT2i_2018
187 beta_LT12_HT4i_NB2_NJ68_NT1_CR_2018
106 +10 −9
188 kappa_LT12_HT03_NB2_NJ68_NT1_2017
189 beta_LT12_HT4i_NB3i_NJ9i_NT2i_CR_2017
6.0 +2.7 −2.0
190 beta_LT3_HT03i_NB3i_NJ68_NT2i_CR_2017
6.0 +2.7 −2.1
191 beta_LT12_HT03_NB1_NJ68_NT2i_CR_2017
118 +11 −10
192 gamma_LT12_HT03_NB2i_NJ45f6_NT1i_SR_2016
142 +5 −5
193 delta_LT12_HT03_NB2i_NJ45f9_NT1i_CR_2017
3770 +31 −30
194 kappa_LT3_HT03i_NB3i_NJ68_NT2i_2016
195 kappa_LT4i_HT03i_NB1_NJ68_NT2i_2017
196 delta_LT12_HT03_NB2i_NJ45f9_NT1i_CR_2016
3333 +29 −29
197 delta_LT4i_HT03i_NB1i_NJ45f9_NT1i_CR_2018
460 +12 −12
198 beta_LT4i_HT03i_NB1_NJ68_NT1_CR_2018
125 +11 −11
199 kappa_LT4i_HT03i_NB1_NJ68_NT2i_2018
200 delta_LT3_HT03i_NB2i_NJ45f9_NT1i_CR_2018
715 +15 −15
201 deltadata_QCDpred_LT12_HT03_NB1_NJ45f6_NT1i_CR_2018
202 delta_LT12_HT4i_NB1i_NJ45f6_NT1i_CR_2016
117 +4 −4
203 delta_LT4i_HT03i_NB1i_NJ45f9_NT1i_CR_2016
295 +10 −10
204 kappa_LT12_HT03_NB2_NJ68_NT1_2016
205 kappa_LT12_HT03_NB2_NJ9i_NT1_2018
206 beta_LT4i_HT03i_NB2_NJ68_NT1_CR_2016
52 +7 −7
207 kappa_LT3_HT03i_NB1_NJ68_NT2i_2017
208 betadata_QCDpred_LT4i_HT03i_NB3i_NJ9i_NT1i_CR_2018
209 beta_LT4i_HT03i_NB3i_NJ68_NT2i_CR_2017
1.0 +1.3 −0.7
210 beta_LT12_HT4i_NB1_NJ68_NT2i_CR_2018
15.0 +3.9 −3.3
−2
−1
0
1
2
−0.001
0
0.001
Pull
+1σ Impact
-1σ Impact
(θ̂-θ0)/Δθ
Δr̂

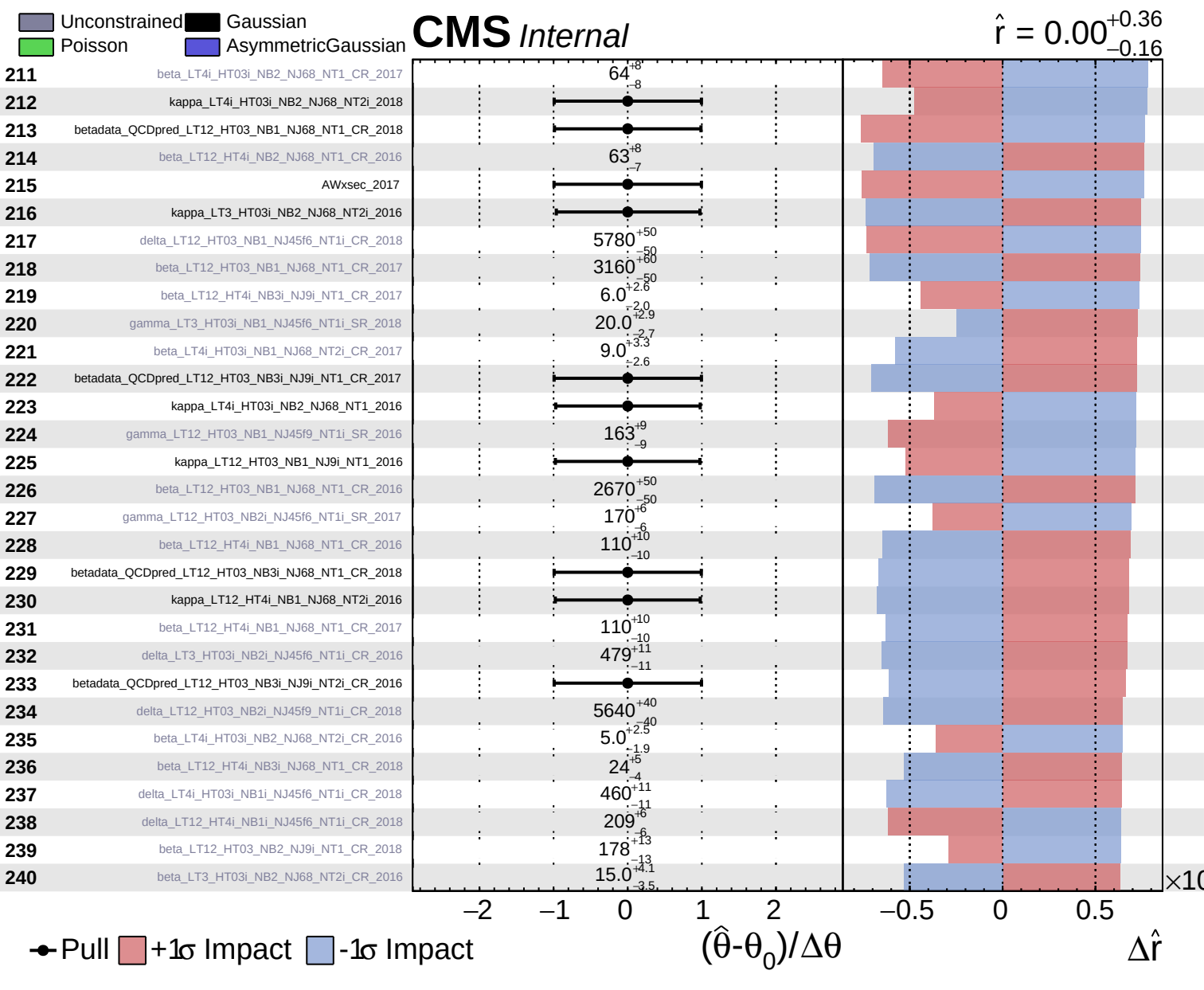
Unconstrained
Gaussian
Poisson
AsymmetricGaussian
CMS Internal
r̂ = 0.00 +0.36 −0.16
211 beta_LT4i_HT03i_NB2_NJ68_NT1_CR_2017
212 kappa_LT4i_HT03i_NB2_NJ68_NT2i_2018
213 betadata_QCDpred_LT12_HT03_NB1_NJ68_NT1_CR_2018
214 beta_LT12_HT4i_NB2_NJ68_NT1_CR_2016
215 AWxsec_2017
216 kappa_LT3_HT03i_NB2_NJ68_NT2i_2016
217 delta_LT12_HT03_NB1_NJ45f6_NT1i_CR_2018
218 beta_LT12_HT03_NB1_NJ68_NT1_CR_2017
219 beta_LT12_HT4i_NB3i_NJ9i_NT1_CR_2017
220 gamma_LT3_HT03i_NB1_NJ45f6_NT1i_SR_2018
221 beta_LT4i_HT03i_NB1_NJ68_NT2i_CR_2017
222 betadata_QCDpred_LT12_HT03_NB3i_NJ9i_NT1_CR_2017
223 kappa_LT4i_HT03i_NB2_NJ68_NT1_2016
224 gamma_LT12_HT03_NB1_NJ45f9_NT1i_SR_2016
225 kappa_LT12_HT03_NB1_NJ9i_NT1_2016
226 beta_LT12_HT03_NB1_NJ68_NT1_CR_2016
227 gamma_LT12_HT03_NB2i_NJ45f6_NT1i_SR_2017
228 beta_LT12_HT4i_NB1_NJ68_NT1_CR_2016
229 betadata_QCDpred_LT12_HT03_NB3i_NJ68_NT1_CR_2018
230 kappa_LT12_HT4i_NB1_NJ68_NT2i_2016
231 beta_LT12_HT4i_NB1_NJ68_NT1_CR_2017
232 delta_LT3_HT03i_NB2i_NJ45f6_NT1i_CR_2016
233 betadata_QCDpred_LT12_HT03_NB3i_NJ9i_NT2i_CR_2016
234 delta_LT12_HT03_NB2i_NJ45f9_NT1i_CR_2018
235 beta_LT4i_HT03i_NB2_NJ68_NT2i_CR_2016
236 beta_LT12_HT4i_NB3i_NJ68_NT1_CR_2018
237 delta_LT4i_HT03i_NB1i_NJ45f6_NT1i_CR_2018
238 delta_LT12_HT4i_NB1i_NJ45f6_NT1i_CR_2018
239 beta_LT12_HT03_NB2_NJ9i_NT1_CR_2018
240 beta_LT3_HT03i_NB2_NJ68_NT2i_CR_2016
64 +8 −8
63 +8 −7
5780 +50 −50
3160 +60 −50
6.0 +2.6 −2.0
20.0 +2.9 −2.7
9.0 +3.3 −2.6
163 +9 −9
2670 +50 −50
170 +6 −6
110 +10 −10
110 +10 −10
479 +11 −11
5640 +40 −40
5.0 +2.5 −1.9
24 +5 −4
460 +11 −11
209 +6 −6
178 +13 −13
15.0 +4.1 −3.5
×10
−2 −1 0 1 2
−0.5 0 0.5
Pull
+1σ Impact
-1σ Impact
(θ̂-θ0)/Δθ
Δr̂

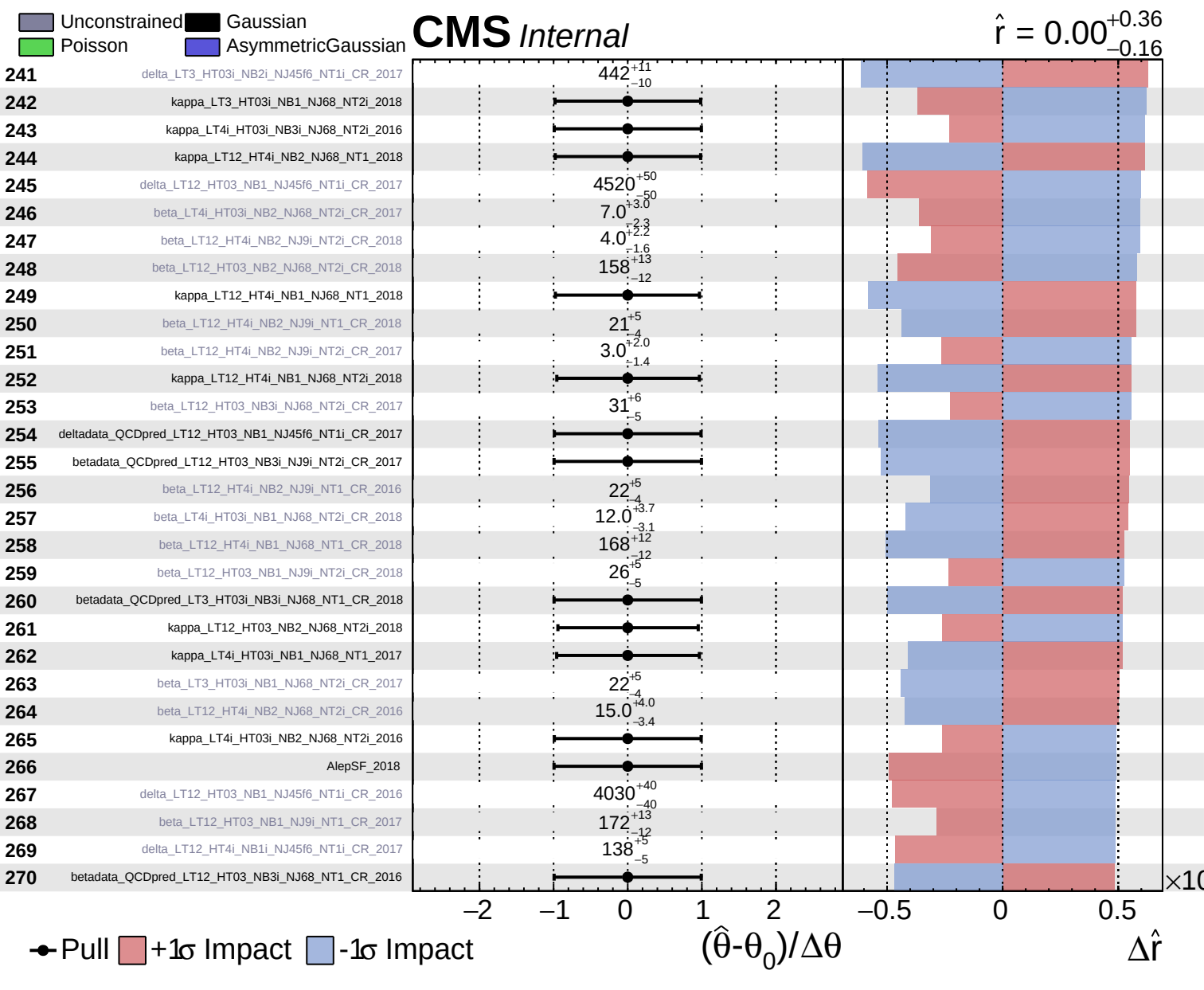
Unconstrained
Gaussian
Poisson
AsymmetricGaussian
CMS Internal
r̂ = 0.00 +0.36 −0.16
241 delta_LT3_HT03i_NB2i_NJ45f6_NT1i_CR_2017
242 kappa_LT3_HT03i_NB1_NJ68_NT2i_2018
243 kappa_LT4i_HT03i_NB3i_NJ68_NT2i_2016
244 kappa_LT12_HT4i_NB2_NJ68_NT1_2018
245 delta_LT12_HT03_NB1_NJ45f6_NT1i_CR_2017
246 beta_LT4i_HT03i_NB2_NJ68_NT2i_CR_2017
247 beta_LT12_HT4i_NB2_NJ9i_NT2i_CR_2018
248 beta_LT12_HT03_NB2_NJ68_NT2i_CR_2018
249 kappa_LT12_HT4i_NB1_NJ68_NT1_2018
250 beta_LT12_HT4i_NB2_NJ9i_NT1_CR_2018
251 beta_LT12_HT4i_NB2_NJ9i_NT2i_CR_2017
252 kappa_LT12_HT4i_NB1_NJ68_NT2i_2018
253 beta_LT12_HT03_NB3i_NJ68_NT2i_CR_2017
254 deltadata_QCDpred_LT12_HT03_NB1_NJ45f6_NT1i_CR_2017
255 betadata_QCDpred_LT12_HT03_NB3i_NJ9i_NT2i_CR_2017
256 beta_LT12_HT4i_NB2_NJ9i_NT1_CR_2016
257 beta_LT4i_HT03i_NB1_NJ68_NT2i_CR_2018
258 beta_LT12_HT4i_NB1_NJ68_NT1_CR_2018
259 beta_LT12_HT03_NB1_NJ9i_NT2i_CR_2018
260 betadata_QCDpred_LT3_HT03i_NB3i_NJ68_NT1_CR_2018
261 kappa_LT12_HT03_NB2_NJ68_NT2i_2018
262 kappa_LT4i_HT03i_NB1_NJ68_NT1_2017
263 beta_LT3_HT03i_NB1_NJ68_NT2i_CR_2017
264 beta_LT12_HT4i_NB2_NJ68_NT2i_CR_2016
265 kappa_LT4i_HT03i_NB2_NJ68_NT2i_2016
266 AlepSF_2018
267 delta_LT12_HT03_NB1_NJ45f6_NT1i_CR_2016
268 beta_LT12_HT03_NB1_NJ9i_NT1_CR_2017
269 delta_LT12_HT4i_NB1i_NJ45f6_NT1i_CR_2017
270 betadata_QCDpred_LT12_HT03_NB3i_NJ68_NT1_CR_2016
442 +11 −10
4520 +50 −50
7.0 +3.0 −2.3
4.0 +2.2 −1.6
158 +13 −12
21 +5 −4
3.0 +2.0 −1.4
31 +6 −5
22 +5 −4
12.0 +3.7 −3.1
168 +12 −12
26 +5 −5
22 +5 −4
15.0 +4.0 −3.4
4030 +40 −40
172 +13 −12
138 +5 −5
−2 −1 0 1 2
−0.5 0 0.5
×10
Pull
+1σ Impact
-1σ Impact
(θ̂-θ0)/Δθ
Δr̂

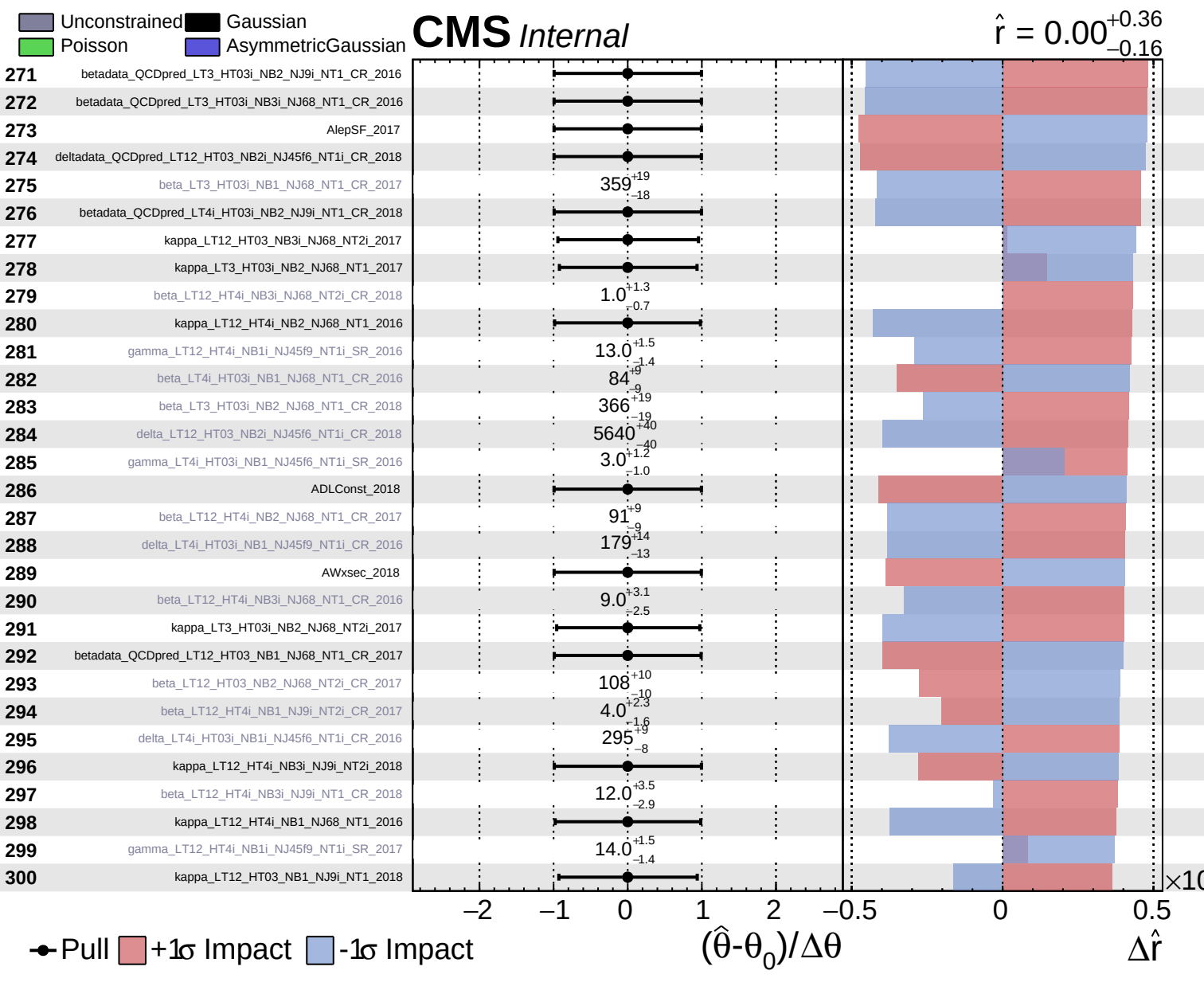
Unconstrained
Gaussian
Poisson
AsymmetricGaussian
CMS Internal
r̂ = 0.00 +0.36 −0.16
271 betadata_QCDpred_LT3_HT03i_NB2_NJ9i_NT1_CR_2016
272 betadata_QCDpred_LT3_HT03i_NB3i_NJ68_NT1_CR_2016
273 AlepSF_2017
274 deltadata_QCDpred_LT12_HT03_NB2i_NJ45f6_NT1i_CR_2018
275 beta_LT3_HT03i_NB1_NJ68_NT1_CR_2017
359 +19 −18
276 betadata_QCDpred_LT4i_HT03i_NB2_NJ9i_NT1_CR_2018
277 kappa_LT12_HT03_NB3i_NJ68_NT2i_2017
278 kappa_LT3_HT03i_NB2_NJ68_NT1_2017
279 beta_LT12_HT4i_NB3i_NJ68_NT2i_CR_2018
1.0 +1.3 −0.7
280 kappa_LT12_HT4i_NB2_NJ68_NT1_2016
281 gamma_LT12_HT4i_NB1i_NJ45f9_NT1i_SR_2016
13.0 +1.5 −1.4
282 beta_LT4i_HT03i_NB1_NJ68_NT1_CR_2016
84 +9 −9
283 beta_LT3_HT03i_NB2_NJ68_NT1_CR_2018
366 +19 −19
284 delta_LT12_HT03_NB2i_NJ45f6_NT1i_CR_2018
5640 +40 −40
285 gamma_LT4i_HT03i_NB1_NJ45f6_NT1i_SR_2016
3.0 +1.2 −1.0
286 ADLConst_2018
287 beta_LT12_HT4i_NB2_NJ68_NT1_CR_2017
91 +9 −9
288 delta_LT4i_HT03i_NB1_NJ45f9_NT1i_CR_2016
179 +14 −13
289 AWxsec_2018
290 beta_LT12_HT4i_NB3i_NJ68_NT1_CR_2016
9.0 +3.1 −2.5
291 kappa_LT3_HT03i_NB2_NJ68_NT2i_2017
292 betadata_QCDpred_LT12_HT03_NB1_NJ68_NT1_CR_2017
293 beta_LT12_HT03_NB2_NJ68_NT2i_CR_2017
108 +10 −10
294 beta_LT12_HT4i_NB1_NJ9i_NT2i_CR_2017
4.0 +2.3 −1.6
295 delta_LT4i_HT03i_NB1i_NJ45f6_NT1i_CR_2016
295 +9 −8
296 kappa_LT12_HT4i_NB3i_NJ9i_NT2i_2018
297 beta_LT12_HT4i_NB3i_NJ9i_NT1_CR_2018
12.0 +3.5 −2.9
298 kappa_LT12_HT4i_NB1_NJ68_NT1_2016
299 gamma_LT12_HT4i_NB1i_NJ45f9_NT1i_SR_2017
14.0 +1.5 −1.4
300 kappa_LT12_HT03_NB1_NJ9i_NT1_2018
×10
−2 −1 0 1 2
−0.5 0 0.5
Pull
+1σ Impact
-1σ Impact
(θ̂-θ0)/Δθ
Δr̂

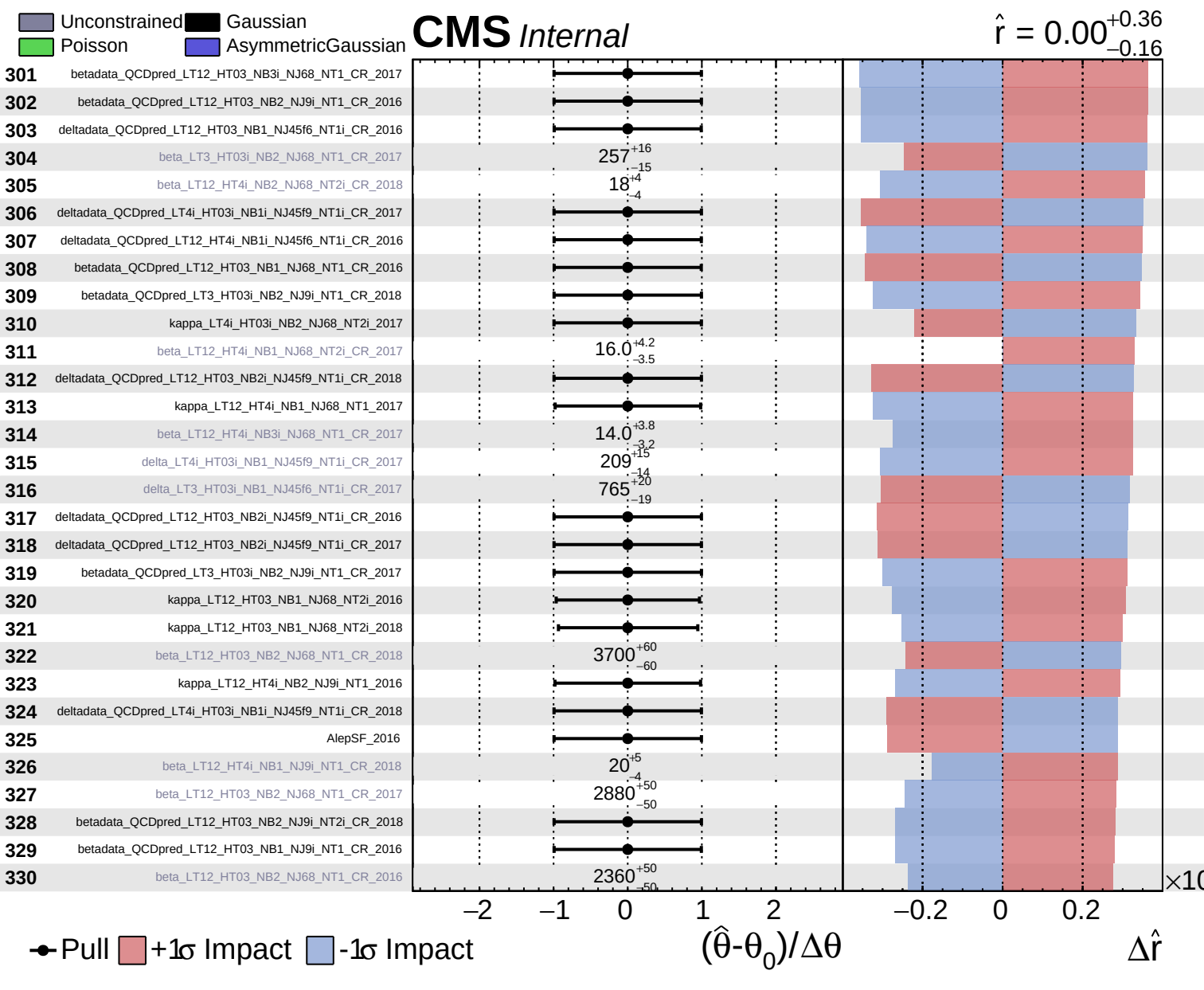
Unconstrained
Gaussian
Poisson
AsymmetricGaussian
CMS Internal
r̂ = 0.00 +0.36 −0.16
301 betadata_QCDpred_LT12_HT03_NB3i_NJ68_NT1_CR_2017
302 betadata_QCDpred_LT12_HT03_NB2_NJ9i_NT1_CR_2016
303 deltadata_QCDpred_LT12_HT03_NB1_NJ45f6_NT1i_CR_2016
304 beta_LT3_HT03i_NB2_NJ68_NT1_CR_2017
257 +16 −15
305 beta_LT12_HT4i_NB2_NJ68_NT2i_CR_2018
18 +4 −4
306 deltadata_QCDpred_LT4i_HT03i_NB1i_NJ45f9_NT1i_CR_2017
307 deltadata_QCDpred_LT12_HT4i_NB1i_NJ45f6_NT1i_CR_2016
308 betadata_QCDpred_LT12_HT03_NB1_NJ68_NT1_CR_2016
309 betadata_QCDpred_LT3_HT03i_NB2_NJ9i_NT1_CR_2018
310 kappa_LT4i_HT03i_NB2_NJ68_NT2i_2017
311 beta_LT12_HT4i_NB1_NJ68_NT2i_CR_2017
16.0 +4.2 −3.5
312 deltadata_QCDpred_LT12_HT03_NB2i_NJ45f9_NT1i_CR_2018
313 kappa_LT12_HT4i_NB1_NJ68_NT1_2017
314 beta_LT12_HT4i_NB3i_NJ68_NT1_CR_2017
14.0 +3.8 −3.2
315 delta_LT4i_HT03i_NB1_NJ45f9_NT1i_CR_2017
209 +15 −14
316 delta_LT3_HT03i_NB1_NJ45f6_NT1i_CR_2017
765 +20 −19
317 deltadata_QCDpred_LT12_HT03_NB2i_NJ45f9_NT1i_CR_2016
318 deltadata_QCDpred_LT12_HT03_NB2i_NJ45f9_NT1i_CR_2017
319 betadata_QCDpred_LT3_HT03i_NB2_NJ9i_NT1_CR_2017
320 kappa_LT12_HT03_NB1_NJ68_NT2i_2016
321 kappa_LT12_HT03_NB1_NJ68_NT2i_2018
322 beta_LT12_HT03_NB2_NJ68_NT1_CR_2018
3700 +60 −60
323 kappa_LT12_HT4i_NB2_NJ9i_NT1_2016
324 deltadata_QCDpred_LT4i_HT03i_NB1i_NJ45f9_NT1i_CR_2018
325 AlepSF_2016
326 beta_LT12_HT4i_NB1_NJ9i_NT1_CR_2018
20 +5 −4
327 beta_LT12_HT03_NB2_NJ68_NT1_CR_2017
2880 +50 −50
328 betadata_QCDpred_LT12_HT03_NB2_NJ9i_NT2i_CR_2018
329 betadata_QCDpred_LT12_HT03_NB1_NJ9i_NT1_CR_2016
330 beta_LT12_HT03_NB2_NJ68_NT1_CR_2016
2360 +50 −50
×10
−2 −1 0 1 2
−0.2 0 0.2
Pull +1σ Impact -1σ Impact
(θ̂-θ0)/Δθ
Δr̂

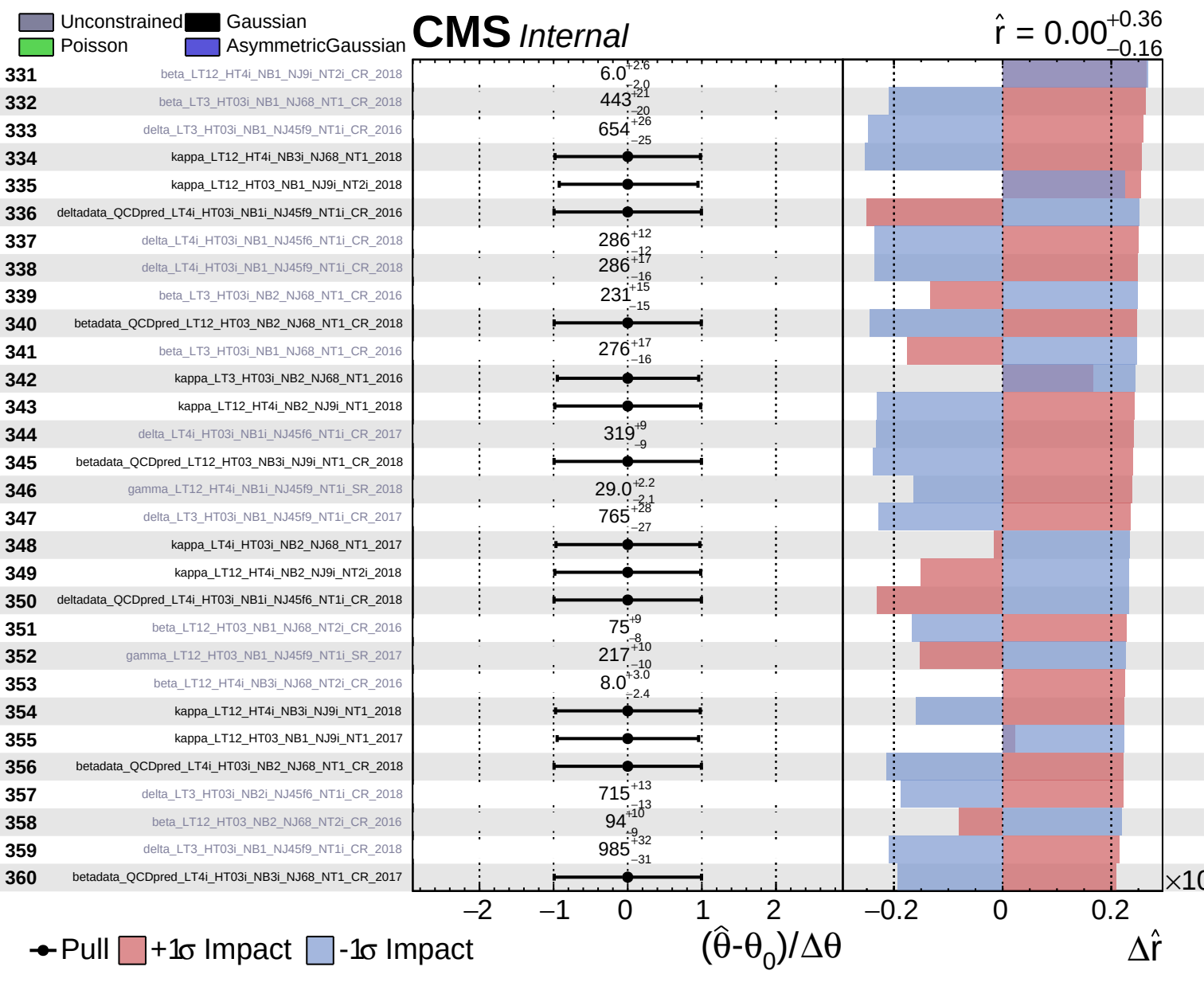
Unconstrained
Gaussian
Poisson
AsymmetricGaussian
CMS Internal
r̂ = 0.00 +0.36 −0.16
331 beta_LT12_HT4i_NB1_NJ9i_NT2i_CR_2018
6.0 +2.6 −2.0
332 beta_LT3_HT03i_NB1_NJ68_NT1_CR_2018
443 +21 −20
333 delta_LT3_HT03i_NB1_NJ45f9_NT1i_CR_2016
654 +26 −25
334 kappa_LT12_HT4i_NB3i_NJ68_NT1_2018
335 kappa_LT12_HT03_NB1_NJ9i_NT2i_2018
336 deltadata_QCDpred_LT4i_HT03i_NB1i_NJ45f9_NT1i_CR_2016
337 delta_LT4i_HT03i_NB1_NJ45f6_NT1i_CR_2018
286 +12 −12
338 delta_LT4i_HT03i_NB1_NJ45f9_NT1i_CR_2018
286 +17 −16
339 beta_LT3_HT03i_NB2_NJ68_NT1_CR_2016
231 +15 −15
340 betadata_QCDpred_LT12_HT03_NB2_NJ68_NT1_CR_2018
341 beta_LT3_HT03i_NB1_NJ68_NT1_CR_2016
276 +17 −16
342 kappa_LT3_HT03i_NB2_NJ68_NT1_2016
343 kappa_LT12_HT4i_NB2_NJ9i_NT1_2018
344 delta_LT4i_HT03i_NB1i_NJ45f6_NT1i_CR_2017
319 +9 −9
345 betadata_QCDpred_LT12_HT03_NB3i_NJ9i_NT1_CR_2018
346 gamma_LT12_HT4i_NB1i_NJ45f9_NT1i_SR_2018
29.0 +2.2 −2.1
347 delta_LT3_HT03i_NB1_NJ45f9_NT1i_CR_2017
765 +28 −27
348 kappa_LT4i_HT03i_NB2_NJ68_NT1_2017
349 kappa_LT12_HT4i_NB2_NJ9i_NT2i_2018
350 deltadata_QCDpred_LT4i_HT03i_NB1i_NJ45f6_NT1i_CR_2018
351 beta_LT12_HT03_NB1_NJ68_NT2i_CR_2016
75 +9 −8
352 gamma_LT12_HT03_NB1_NJ45f9_NT1i_SR_2017
217 +10 −10
353 beta_LT12_HT4i_NB3i_NJ68_NT2i_CR_2016
8.0 +3.0 −2.4
354 kappa_LT12_HT4i_NB3i_NJ9i_NT1_2018
355 kappa_LT12_HT03_NB1_NJ9i_NT1_2017
356 betadata_QCDpred_LT4i_HT03i_NB2_NJ68_NT1_CR_2018
357 delta_LT3_HT03i_NB2i_NJ45f6_NT1i_CR_2018
715 +13 −13
358 beta_LT12_HT03_NB2_NJ68_NT2i_CR_2016
94 +10 −9
359 delta_LT3_HT03i_NB1_NJ45f9_NT1i_CR_2018
985 +32 −31
360 betadata_QCDpred_LT4i_HT03i_NB3i_NJ68_NT1_CR_2017
×10
−2
−1
0
1
2
−0.2
0
0.2
Pull
+1σ Impact
-1σ Impact
(θ̂-θ0)/Δθ
Δr̂

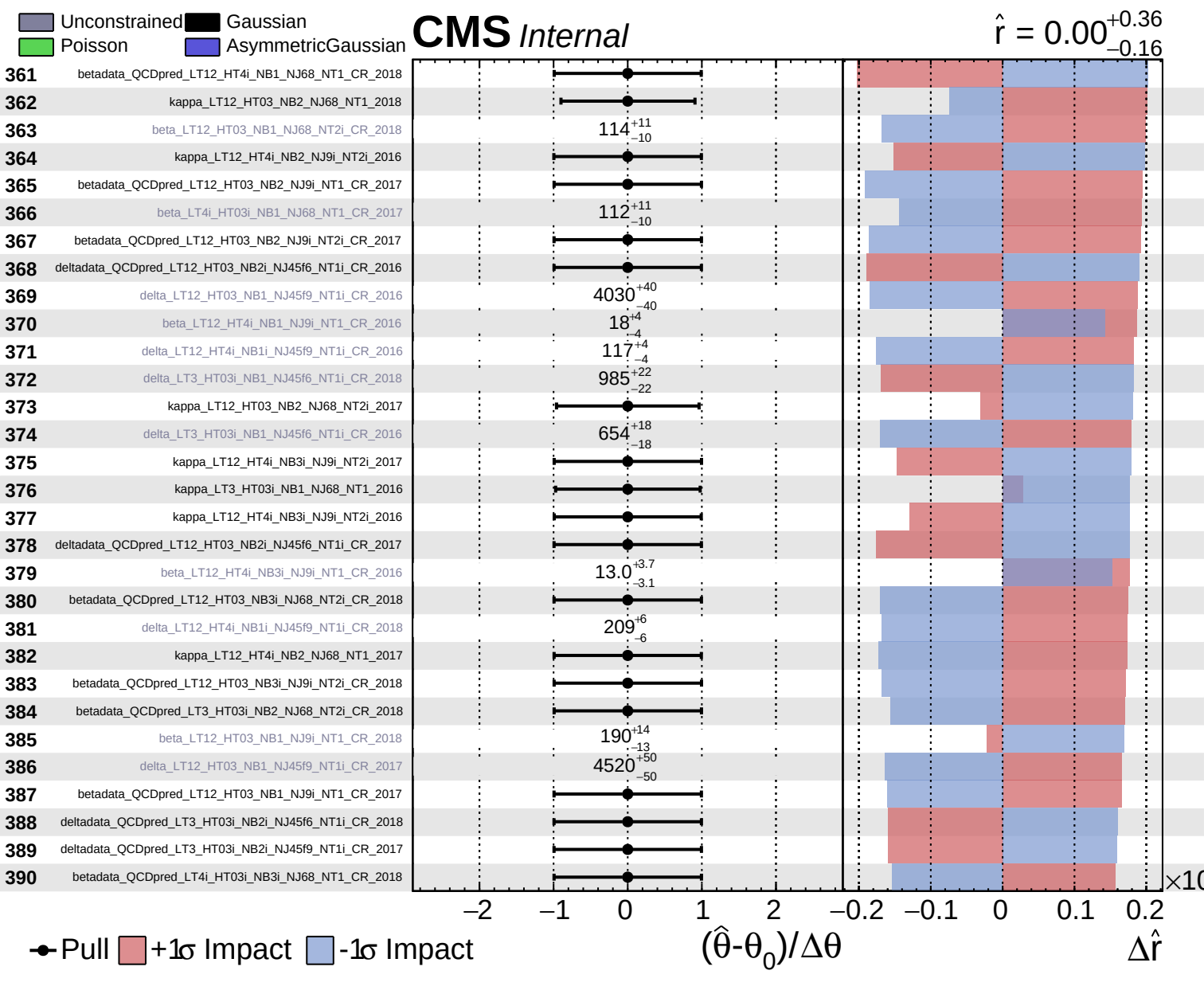
Unconstrained
Gaussian
Poisson
AsymmetricGaussian
CMS Internal
r̂ = 0.00 +0.36 −0.16
361 betadata_QCDpred_LT12_HT4i_NB1_NJ68_NT1_CR_2018
362 kappa_LT12_HT03_NB2_NJ68_NT1_2018
363 beta_LT12_HT03_NB1_NJ68_NT2i_CR_2018
364 kappa_LT12_HT4i_NB2_NJ9i_NT2i_2016
365 betadata_QCDpred_LT12_HT03_NB2_NJ9i_NT1_CR_2017
366 beta_LT4i_HT03i_NB1_NJ68_NT1_CR_2017
367 betadata_QCDpred_LT12_HT03_NB2_NJ9i_NT2i_CR_2017
368 deltadata_QCDpred_LT12_HT03_NB2i_NJ45f6_NT1i_CR_2016
369 delta_LT12_HT03_NB1_NJ45f9_NT1i_CR_2016
370 beta_LT12_HT4i_NB1_NJ9i_NT1_CR_2016
371 delta_LT12_HT4i_NB1i_NJ45f9_NT1i_CR_2016
372 delta_LT3_HT03i_NB1_NJ45f6_NT1i_CR_2018
373 kappa_LT12_HT03_NB2_NJ68_NT2i_2017
374 delta_LT3_HT03i_NB1_NJ45f6_NT1i_CR_2016
375 kappa_LT12_HT4i_NB3i_NJ9i_NT2i_2017
376 kappa_LT3_HT03i_NB1_NJ68_NT1_2016
377 kappa_LT12_HT4i_NB3i_NJ9i_NT2i_2016
378 deltadata_QCDpred_LT12_HT03_NB2i_NJ45f6_NT1i_CR_2017
379 beta_LT12_HT4i_NB3i_NJ9i_NT1_CR_2016
380 betadata_QCDpred_LT12_HT03_NB3i_NJ68_NT2i_CR_2018
381 delta_LT12_HT4i_NB1i_NJ45f9_NT1i_CR_2018
382 kappa_LT12_HT4i_NB2_NJ68_NT1_2017
383 betadata_QCDpred_LT12_HT03_NB3i_NJ9i_NT2i_CR_2018
384 betadata_QCDpred_LT3_HT03i_NB2_NJ68_NT2i_CR_2018
385 beta_LT12_HT03_NB1_NJ9i_NT1_CR_2018
386 delta_LT12_HT03_NB1_NJ45f9_NT1i_CR_2017
387 betadata_QCDpred_LT12_HT03_NB1_NJ9i_NT1_CR_2017
388 deltadata_QCDpred_LT3_HT03i_NB2i_NJ45f6_NT1i_CR_2018
389 deltadata_QCDpred_LT3_HT03i_NB2i_NJ45f9_NT1i_CR_2017
390 betadata_QCDpred_LT4i_HT03i_NB3i_NJ68_NT1_CR_2018
114 +11 −10
112 +11 −10
4030 +40 −40
18 +4 −4
117 +4 −4
985 +22 −22
654 +18 −18
13.0 +3.7 −3.1
209 +6 −6
190 +14 −13
4520 +50 −50
×10
−2 −1 0 1 2
−0.2 −0.1 0 0.1 0.2
Pull
+1σ Impact
-1σ Impact
(θ̂-θ0)/Δθ
Δr̂

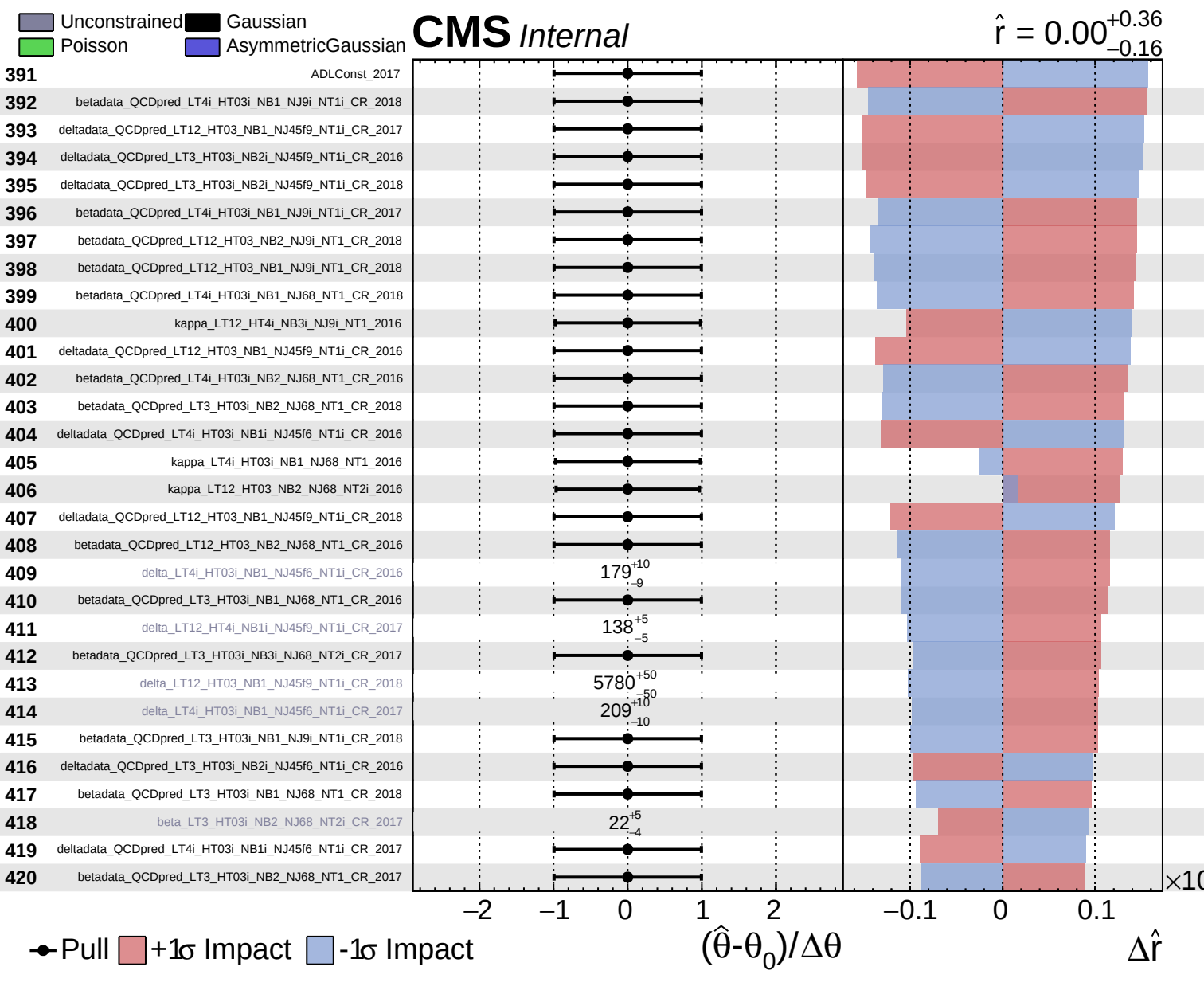
Unconstrained
Gaussian
Poisson
AsymmetricGaussian
CMS Internal
r̂ = 0.00 +0.36 −0.16
391 ADLConst_2017
392 betadata_QCDpred_LT4i_HT03i_NB1_NJ9i_NT1i_CR_2018
393 deltadata_QCDpred_LT12_HT03_NB1_NJ45f9_NT1i_CR_2017
394 deltadata_QCDpred_LT3_HT03i_NB2i_NJ45f9_NT1i_CR_2016
395 deltadata_QCDpred_LT3_HT03i_NB2i_NJ45f9_NT1i_CR_2018
396 betadata_QCDpred_LT4i_HT03i_NB1_NJ9i_NT1i_CR_2017
397 betadata_QCDpred_LT12_HT03_NB2_NJ9i_NT1_CR_2018
398 betadata_QCDpred_LT12_HT03_NB1_NJ9i_NT1_CR_2018
399 betadata_QCDpred_LT4i_HT03i_NB1_NJ68_NT1_CR_2018
400 kappa_LT12_HT4i_NB3i_NJ9i_NT1_2016
401 deltadata_QCDpred_LT12_HT03_NB1_NJ45f9_NT1i_CR_2016
402 betadata_QCDpred_LT4i_HT03i_NB2_NJ68_NT1_CR_2016
403 betadata_QCDpred_LT3_HT03i_NB2_NJ68_NT1_CR_2018
404 deltadata_QCDpred_LT4i_HT03i_NB1i_NJ45f6_NT1i_CR_2016
405 kappa_LT4i_HT03i_NB1_NJ68_NT1_2016
406 kappa_LT12_HT03_NB2_NJ68_NT2i_2016
407 deltadata_QCDpred_LT12_HT03_NB1_NJ45f9_NT1i_CR_2018
408 betadata_QCDpred_LT12_HT03_NB2_NJ68_NT1_CR_2016
409 delta_LT4i_HT03i_NB1_NJ45f6_NT1i_CR_2016
179 +10 −9
410 betadata_QCDpred_LT3_HT03i_NB1_NJ68_NT1_CR_2016
411 delta_LT12_HT4i_NB1i_NJ45f9_NT1i_CR_2017
138 +5 −5
412 betadata_QCDpred_LT3_HT03i_NB3i_NJ68_NT2i_CR_2017
413 delta_LT12_HT03_NB1_NJ45f9_NT1i_CR_2018
5780 +50 −50
414 delta_LT4i_HT03i_NB1_NJ45f6_NT1i_CR_2017
209 +10 −10
415 betadata_QCDpred_LT3_HT03i_NB1_NJ9i_NT1i_CR_2018
416 deltadata_QCDpred_LT3_HT03i_NB2i_NJ45f6_NT1i_CR_2016
417 betadata_QCDpred_LT3_HT03i_NB1_NJ68_NT1_CR_2018
418 beta_LT3_HT03i_NB2_NJ68_NT2i_CR_2017
22 +5 −4
419 deltadata_QCDpred_LT4i_HT03i_NB1i_NJ45f6_NT1i_CR_2017
420 betadata_QCDpred_LT3_HT03i_NB2_NJ68_NT1_CR_2017
−2 −1 0 1 2
−0.1 0 0.1
×10
Pull
+1σ Impact
-1σ Impact
(θ̂-θ0)/Δθ
Δr̂

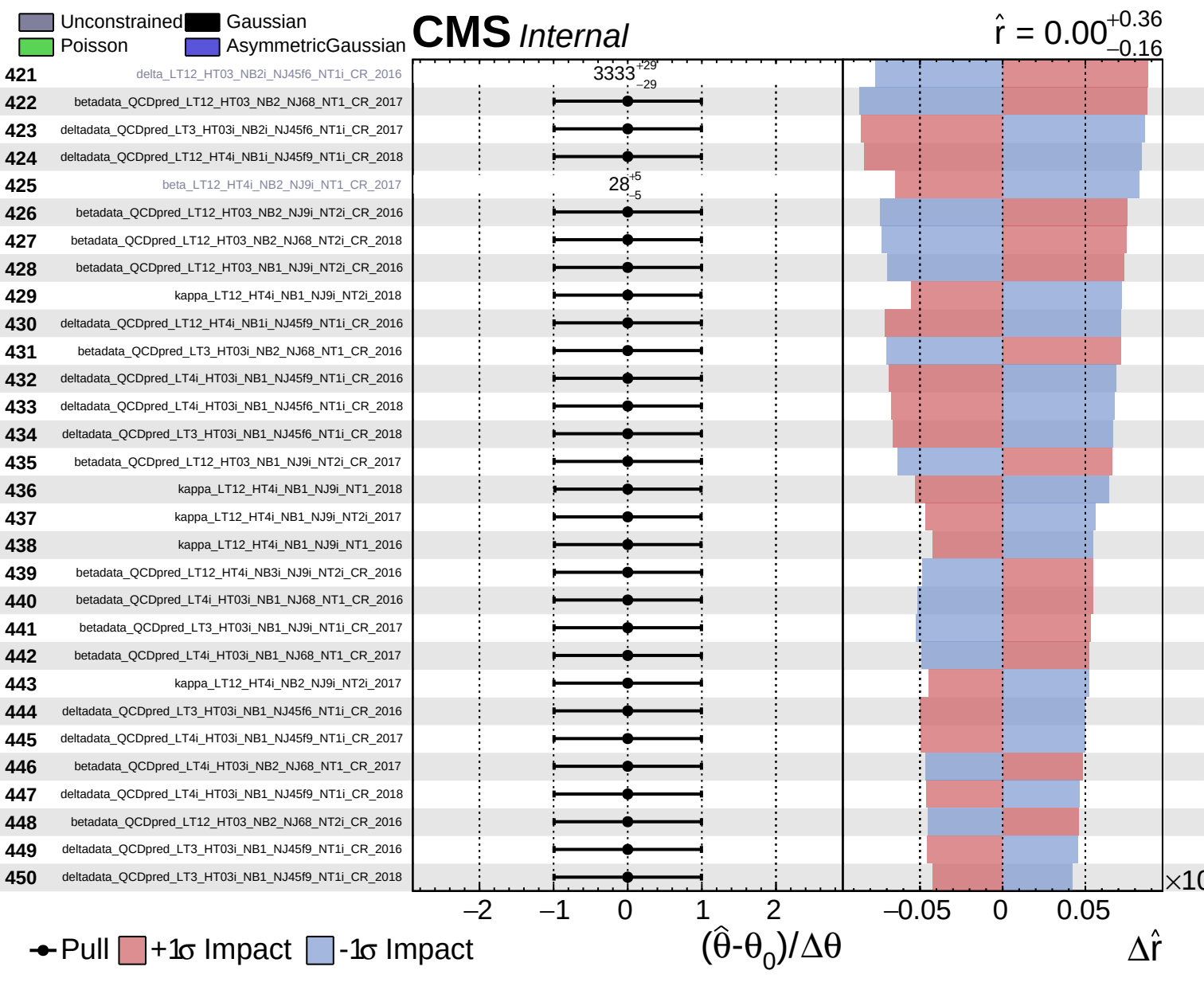
Unconstrained
Gaussian
Poisson
AsymmetricGaussian
CMS Internal
r̂ = 0.00 +0.36 −0.16
421 delta_LT12_HT03_NB2i_NJ45f6_NT1i_CR_2016
422 betadata_QCDpred_LT12_HT03_NB2_NJ68_NT1_CR_2017
423 deltadata_QCDpred_LT3_HT03i_NB2i_NJ45f6_NT1i_CR_2017
424 deltadata_QCDpred_LT12_HT4i_NB1i_NJ45f9_NT1i_CR_2018
425 beta_LT12_HT4i_NB2_NJ9i_NT1_CR_2017
426 betadata_QCDpred_LT12_HT03_NB2_NJ9i_NT2i_CR_2016
427 betadata_QCDpred_LT12_HT03_NB2_NJ68_NT2i_CR_2018
428 betadata_QCDpred_LT12_HT03_NB1_NJ9i_NT2i_CR_2016
429 kappa_LT12_HT4i_NB1_NJ9i_NT2i_2018
430 deltadata_QCDpred_LT12_HT4i_NB1i_NJ45f9_NT1i_CR_2016
431 betadata_QCDpred_LT3_HT03i_NB2_NJ68_NT1_CR_2016
432 deltadata_QCDpred_LT4i_HT03i_NB1_NJ45f9_NT1i_CR_2016
433 deltadata_QCDpred_LT4i_HT03i_NB1_NJ45f6_NT1i_CR_2018
434 deltadata_QCDpred_LT3_HT03i_NB1_NJ45f6_NT1i_CR_2018
435 betadata_QCDpred_LT12_HT03_NB1_NJ9i_NT2i_CR_2017
436 kappa_LT12_HT4i_NB1_NJ9i_NT1_2018
437 kappa_LT12_HT4i_NB1_NJ9i_NT2i_2017
438 kappa_LT12_HT4i_NB1_NJ9i_NT1_2016
439 betadata_QCDpred_LT12_HT4i_NB3i_NJ9i_NT2i_CR_2016
440 betadata_QCDpred_LT4i_HT03i_NB1_NJ68_NT1_CR_2016
441 betadata_QCDpred_LT3_HT03i_NB1_NJ9i_NT1i_CR_2017
442 betadata_QCDpred_LT4i_HT03i_NB1_NJ68_NT1_CR_2017
443 kappa_LT12_HT4i_NB2_NJ9i_NT2i_2017
444 deltadata_QCDpred_LT3_HT03i_NB1_NJ45f6_NT1i_CR_2016
445 deltadata_QCDpred_LT4i_HT03i_NB1_NJ45f9_NT1i_CR_2017
446 betadata_QCDpred_LT4i_HT03i_NB2_NJ68_NT1_CR_2017
447 deltadata_QCDpred_LT4i_HT03i_NB1_NJ45f9_NT1i_CR_2018
448 betadata_QCDpred_LT12_HT03_NB2_NJ68_NT2i_CR_2016
449 deltadata_QCDpred_LT3_HT03i_NB1_NJ45f9_NT1i_CR_2016
450 deltadata_QCDpred_LT3_HT03i_NB1_NJ45f9_NT1i_CR_2018
3333 +29 −29
28 +5 −5
×10
−2
−1
0
1
2
−0.05
0
0.05
Pull
+1σ Impact
-1σ Impact
(θ̂-θ0)/Δθ
Δr̂

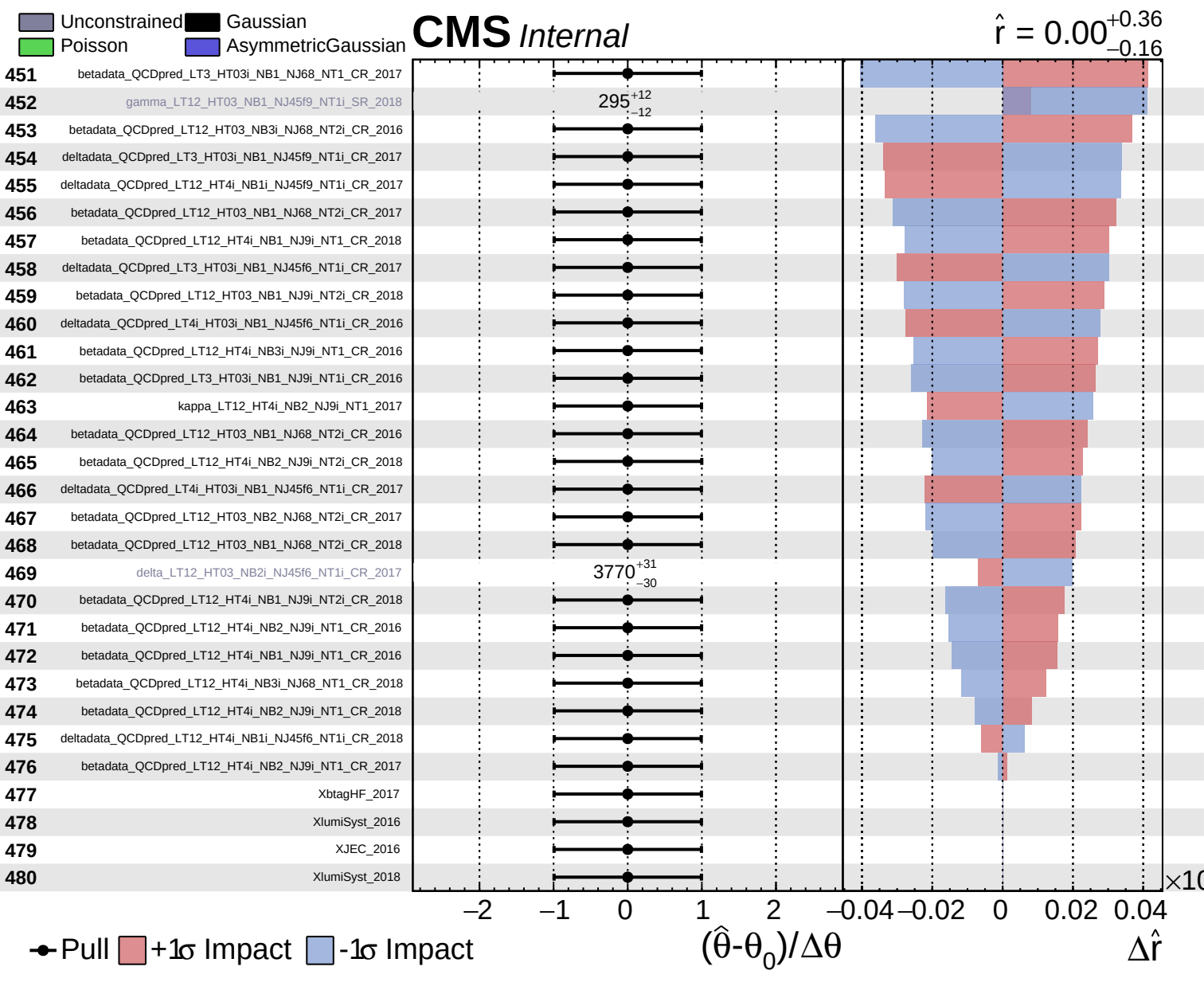
Unconstrained
Gaussian
Poisson
AsymmetricGaussian
CMS Internal
r̂ = 0.00 +0.36 −0.16
451 betadata_QCDpred_LT3_HT03i_NB1_NJ68_NT1_CR_2017
452 gamma_LT12_HT03_NB1_NJ45f9_NT1i_SR_2018
453 betadata_QCDpred_LT12_HT03_NB3i_NJ68_NT2i_CR_2016
454 deltadata_QCDpred_LT3_HT03i_NB1_NJ45f9_NT1i_CR_2017
455 deltadata_QCDpred_LT12_HT4i_NB1i_NJ45f9_NT1i_CR_2017
456 betadata_QCDpred_LT12_HT03_NB1_NJ68_NT2i_CR_2017
457 betadata_QCDpred_LT12_HT4i_NB1_NJ9i_NT1_CR_2018
458 deltadata_QCDpred_LT3_HT03i_NB1_NJ45f6_NT1i_CR_2017
459 betadata_QCDpred_LT12_HT03_NB1_NJ9i_NT2i_CR_2018
460 deltadata_QCDpred_LT4i_HT03i_NB1_NJ45f6_NT1i_CR_2016
461 betadata_QCDpred_LT12_HT4i_NB3i_NJ9i_NT1_CR_2016
462 betadata_QCDpred_LT3_HT03i_NB1_NJ9i_NT1i_CR_2016
463 kappa_LT12_HT4i_NB2_NJ9i_NT1_2017
464 betadata_QCDpred_LT12_HT03_NB1_NJ68_NT2i_CR_2016
465 betadata_QCDpred_LT12_HT4i_NB2_NJ9i_NT2i_CR_2018
466 deltadata_QCDpred_LT4i_HT03i_NB1_NJ45f6_NT1i_CR_2017
467 betadata_QCDpred_LT12_HT03_NB2_NJ68_NT2i_CR_2017
468 betadata_QCDpred_LT12_HT03_NB1_NJ68_NT2i_CR_2018
469 delta_LT12_HT03_NB2i_NJ45f6_NT1i_CR_2017
470 betadata_QCDpred_LT12_HT4i_NB1_NJ9i_NT2i_CR_2018
471 betadata_QCDpred_LT12_HT4i_NB2_NJ9i_NT1_CR_2016
472 betadata_QCDpred_LT12_HT4i_NB1_NJ9i_NT1_CR_2016
473 betadata_QCDpred_LT12_HT4i_NB3i_NJ68_NT1_CR_2018
474 betadata_QCDpred_LT12_HT4i_NB2_NJ9i_NT1_CR_2018
475 deltadata_QCDpred_LT12_HT4i_NB1i_NJ45f6_NT1i_CR_2018
476 betadata_QCDpred_LT12_HT4i_NB2_NJ9i_NT1_CR_2017
477 XbtagHF_2017
478 XlumiSyst_2016
479 XJEC_2016
480 XlumiSyst_2018
295 +12 −12
3770 +31 −30
×10
−2 −1 0 1 2
−0.04 −0.02 0 0.02 0.04
Pull
+1σ Impact
-1σ Impact
(θ̂-θ0)/Δθ
Δr̂

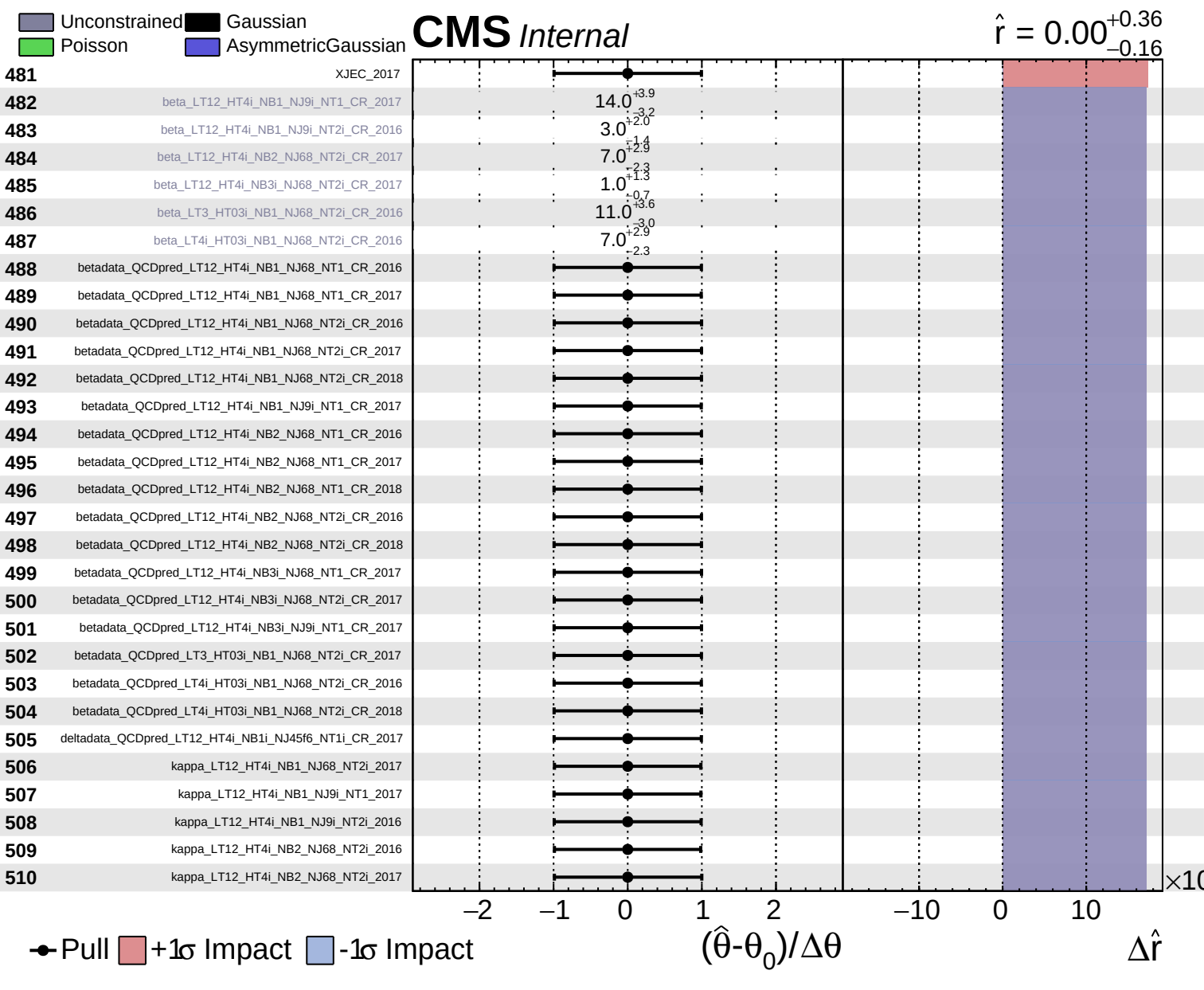
Unconstrained
Gaussian
Poisson
AsymmetricGaussian
CMS Internal
r̂ = 0.00 +0.36 −0.16
481 XJEC_2017
482 beta_LT12_HT4i_NB1_NJ9i_NT1_CR_2017
483 beta_LT12_HT4i_NB1_NJ9i_NT2i_CR_2016
484 beta_LT12_HT4i_NB2_NJ68_NT2i_CR_2017
485 beta_LT12_HT4i_NB3i_NJ68_NT2i_CR_2017
486 beta_LT3_HT03i_NB1_NJ68_NT2i_CR_2016
487 beta_LT4i_HT03i_NB1_NJ68_NT2i_CR_2016
14.0 +3.9 −3.2
3.0 +2.0 −1.4
7.0 +2.9 −2.3
1.0 +1.3 −0.7
11.0 +3.6 −3.0
7.0 +2.9 −2.3
488 betadata_QCDpred_LT12_HT4i_NB1_NJ68_NT1_CR_2016
489 betadata_QCDpred_LT12_HT4i_NB1_NJ68_NT1_CR_2017
490 betadata_QCDpred_LT12_HT4i_NB1_NJ68_NT2i_CR_2016
491 betadata_QCDpred_LT12_HT4i_NB1_NJ68_NT2i_CR_2017
492 betadata_QCDpred_LT12_HT4i_NB1_NJ68_NT2i_CR_2018
493 betadata_QCDpred_LT12_HT4i_NB1_NJ9i_NT1_CR_2017
494 betadata_QCDpred_LT12_HT4i_NB2_NJ68_NT1_CR_2016
495 betadata_QCDpred_LT12_HT4i_NB2_NJ68_NT1_CR_2017
496 betadata_QCDpred_LT12_HT4i_NB2_NJ68_NT1_CR_2018
497 betadata_QCDpred_LT12_HT4i_NB2_NJ68_NT2i_CR_2016
498 betadata_QCDpred_LT12_HT4i_NB2_NJ68_NT2i_CR_2018
499 betadata_QCDpred_LT12_HT4i_NB3i_NJ68_NT1_CR_2017
500 betadata_QCDpred_LT12_HT4i_NB3i_NJ68_NT2i_CR_2017
501 betadata_QCDpred_LT12_HT4i_NB3i_NJ9i_NT1_CR_2017
502 betadata_QCDpred_LT3_HT03i_NB1_NJ68_NT2i_CR_2017
503 betadata_QCDpred_LT4i_HT03i_NB1_NJ68_NT2i_CR_2016
504 betadata_QCDpred_LT4i_HT03i_NB1_NJ68_NT2i_CR_2018
505 deltadata_QCDpred_LT12_HT4i_NB1i_NJ45f6_NT1i_CR_2017
506 kappa_LT12_HT4i_NB1_NJ68_NT2i_2017
507 kappa_LT12_HT4i_NB1_NJ9i_NT1_2017
508 kappa_LT12_HT4i_NB1_NJ9i_NT2i_2016
509 kappa_LT12_HT4i_NB2_NJ68_NT2i_2016
510 kappa_LT12_HT4i_NB2_NJ68_NT2i_2017
×10
−2 −1 0 1 2
−10 0 10
Pull
+1σ Impact
-1σ Impact
(θ̂-θ0)/Δθ
Δr̂

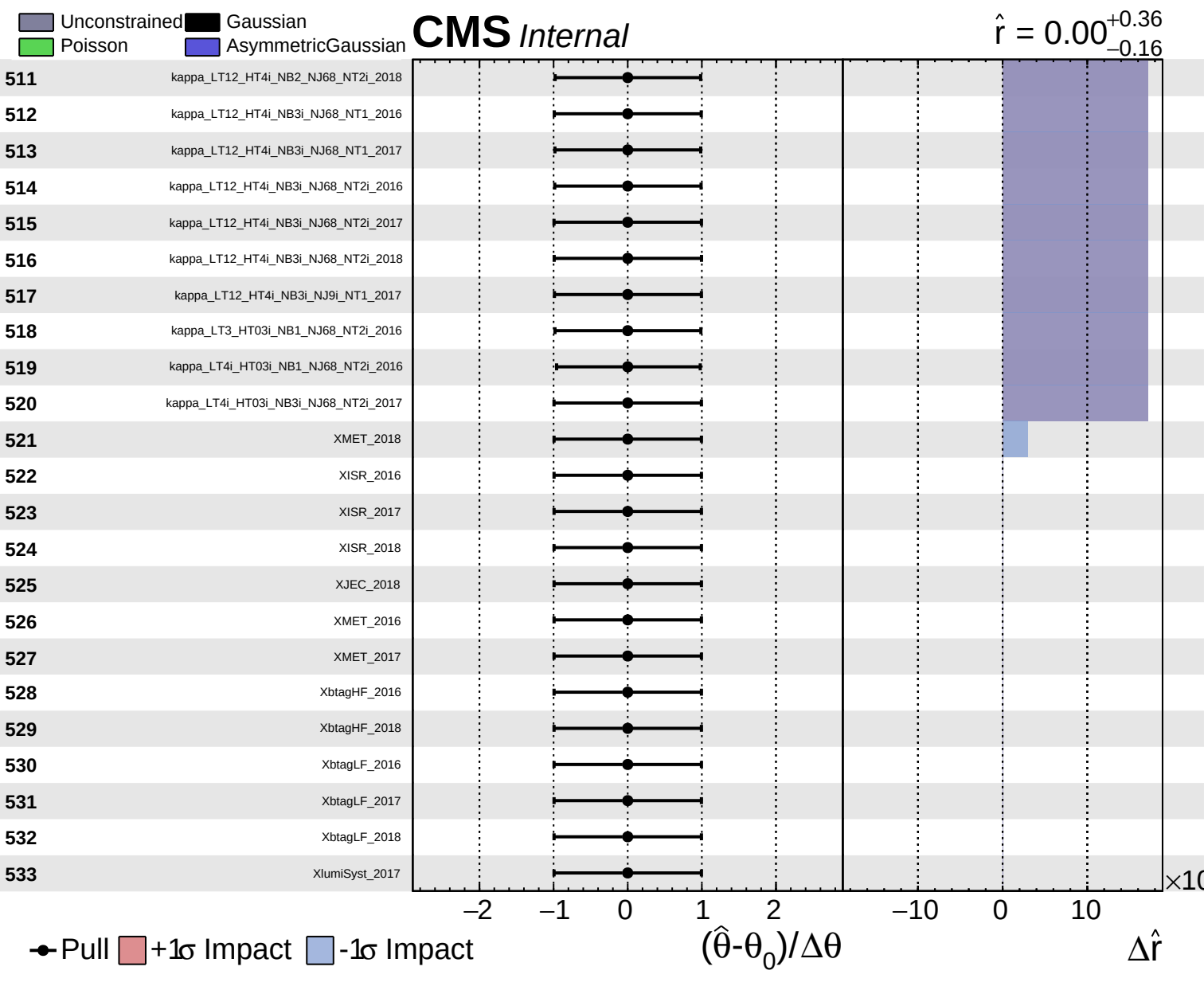
Unconstrained
Gaussian
Poisson
AsymmetricGaussian
CMS Internal
r̂ = 0.00 +0.36 −0.16
511 kappa_LT12_HT4i_NB2_NJ68_NT2i_2018
512 kappa_LT12_HT4i_NB3i_NJ68_NT1_2016
513 kappa_LT12_HT4i_NB3i_NJ68_NT1_2017
514 kappa_LT12_HT4i_NB3i_NJ68_NT2i_2016
515 kappa_LT12_HT4i_NB3i_NJ68_NT2i_2017
516 kappa_LT12_HT4i_NB3i_NJ68_NT2i_2018
517 kappa_LT12_HT4i_NB3i_NJ9i_NT1_2017
518 kappa_LT3_HT03i_NB1_NJ68_NT2i_2016
519 kappa_LT4i_HT03i_NB1_NJ68_NT2i_2016
520 kappa_LT4i_HT03i_NB3i_NJ68_NT2i_2017
521 XMET_2018
522 XISR_2016
523 XISR_2017
524 XISR_2018
525 XJEC_2018
526 XMET_2016
527 XMET_2017
528 XbtagHF_2016
529 XbtagHF_2018
530 XbtagLF_2016
531 XbtagLF_2017
532 XbtagLF_2018
533 XlumiSyst_2017
−2 −1 0 1 2
−10 0 10
×10
Pull
+1σ Impact
-1σ Impact
(θ̂-θ0)/Δθ
Δr̂